Performance Analysis of zeRIS-aided NOMA Communication

Capstone Report

Nurgissa Zhakanov

Nazarbayev University
Department of Electrical and Computer Engineering
School of Engineering and Digital Sciences

This project report was created on TexStudio editing platform using LaTeX. All the figures were drawn using draw.io online software tool.

Electrical and Computer Engineering
Nazarbayev University
http://www.nu.edu.kz

Title:
Performance Analysis of zeRIS-aided NOMA Communication

Theme:
Wireless communication

Project Period:
Fall 2024

Project Group:
Wireless group 3.411

Participant(s):
Nurgissa Zhakanov

Supervisor(s):
Galymzhan Nauryzbayev

Copies: 1

Page Numbers: 37

Date of Completion:
April 25, 2025

Abstract:

This project investigates an innovative method by which wireless communication systems with Non-Orthogonal Multiple Access (NOMA) and zero-energy Reconfigurable Intelligent Surfaces (zeRIS) function together without external power sources. The study presents a thorough performance assessment that includes theoretical and simulated findings. The study shows how zeRIS technology increases system efficiency together with network performance which represents a great sustainable solution for communication infrastructure.

Contents

Preface

The exponential technological advancement in wireless communication system to enhance higher data rate, lower latency and power efficiency has been the main justification for the development of new techniques. From the above mentioned advancements: Non–orthogonal Multiple Access (NOMA) and Reconfigurable intelligent surfaces (RIS). Nevertheless, the integration of these systems creates issues, especially concerning energy viability and system integration.

This work, called Performance Analysis of Zero-Energy RIS (zeRIS)-Aided NOMA Communication, aims to present a new mode where the RIS does not require external energy resources. In this regard, zeRIS, which harvests ambient energy and ensures improved system performances, offers a solution to the sustainable communication networks. Therefore, the project is more about evaluating performance of the system both theoretically and by simulation along with self-sustainable operation of zeRIS.

This research and findings shown in this paper is a demonstration of genuine concern in pushing forward energy efficient wireless communications. This work is the result of a process of learning, testing and cooperation as a step towards the construction of more sustainable technologies in the sector of communication.

For my academic supervisor Dr. Galymzhan Nauryzbayev and other advisors to whom I owe a special word of appreciation, thank you for your support and assistance during my work on this project. This has been the basis of their support in enabling me to undertake and complete this project.

Nazarbayev University, April 25, 2025

Nurgissa Zhakanov
<nurgissa.zhakano@nu.edu.kz>

Chapter 1

Introduction

The surge in connected gadgets like smartphones through to smart homes has posed colossal demands on wireless networks — in fact to a never experienced before level — as we inch towards 5G era and beyond (5GB). The continuous quest for improving wireless technology stems from the need to speedy data transfer rates along with high network capacity and energy efficiency. However, accomplishing such thrilling goals isn't devoid of barriers. Wireless communication poses challenges like small-scale and large-scale fadings, delay, symbol interference, etc.

1.1 Reconfigurable Intelligent Surfaces

One of the solutions to these problems is device known as reconfigurable intelligent surface (RIS). It is equipped with a multitude of tiny, programmable components that can change the amplitude and phase shift of each element [1], [2], [3]. These surfaces are employed to increase the quality of wireless signal or reroute them to facilitate better connection [4], [5]. By reducing interference, boosting signal strength in particular directions, and intelligently regulating signal propagation, RIS is considered a means of optimizing wireless communication. With the advent of 6G and other future wireless communication networks, this idea is very significant [5]. For instance, a conventional passive RIS or single-functional RIS (SF-RIS) reflects an incident signal while simultaneously transmitting and reflecting RIS (STAR-RIS) can reflect and transmit the signal, thus, ensuring full-space coverage [6], [7], [8].

1.2 Active RIS

Double-fading attenuation caused by cascaded channel is mitigated by integrating amplifiers or so-called reflection amplifiers into the RIS [9, 10]. This type of RIS is

termed as an active RIS [11]. However, having a reflection amplifier per unit cell can be inefficient in terms of cost and energy use, especially when the number of unit cells is huge [12, 13]. To this end, [14] and [15] proposed a novel architecture of an active RIS such as sub-connected active RIS which had a common reflection-type amplifier for multiple unit cells. This type of design ensured amplification for all unit cells and reduced their number as well compared to fully-connected active RIS. Nonetheless, both SF-RIS and double-functional RIS (DF-RIS) rely on external power supply such as power grid or battery to maintain a continuous uninterrupted work flow [16], [17], [18].

1.3 Zero-energy RIS

To overcome those problems faced by RISs, a zero-energy RIS (zeRIS), one of the new paradigms, have emerged as an innovative technology that might completely alter wireless communication networks [19], [20]. By leveraging both information and power transmission, RIS can harvest an energy from ambient radio frequency (RF) signals, hence, resulting in zero power consumption at the RIS, [21], [22]. These RISs are known to be as zeRISs or self-sustainable RISs. Because of their exceptional capacity to control electromagnetic waves, these intelligent surfaces have attracted a lot of interest and opened up a range of applications beyond simple communication improvement. To fully appreciate the importance of the zeRIS, it is essential to recognize the difficulties presented by the increasing need for high data rates, low latency communication, and widespread connectivity. Conventional communication infrastructures frequently struggle with energy inefficiency, signal attenuation, and spectrum shortages [23], [1]. As an intelligent mediator that can dynamically adapt to the communication environment, optimize signal propagation, and improve overall network performance, zeRIS emerges as a promising option in this context. zeRIS can harvest energy, reflect and transmit an incident signal simultaneously unlike its predecessors such as SF-RIS or DF-RIS [24], [25]. Hence, zeRIS avoids external power supply and solves the issue of half-space coverage as long as receivers on the other side of the RIS are considered as well [26], [27]. Additionally, a zeRIS can be mounted on walls of the buildings, which substantially facilitated its application in the 5GB by bestowing a convenience on its installation [27].

1.4 Ethical and Professional Responsibilities

1.4.1 Ethical Responsibility

There are some ethical issues concerned with the deployment of a zeRIS like privacy and security as long as the communication system encompasses various different sectors such as governmental, personal, commercial, etc. One the one hand, users should be informed about how their data will be used and stored. On the other hand, a communication must be secure so that eavesdroppers could not access data of users during the transmission through a zeRIS. Therefore, different wireless service providers should take a formal consent from their users to collect and use their data according to local regulations and laws (e.g. Personal Data Law in Kazakhstan or General Data Protection Regulation for European Union). Random checks and transparency reports must be conducted to maintain accountability and trustworthiness. As for security, the message must be robustly encrypted with state-of-the-art techniques such as end-to-end encryption that assures access solely to authorized users. A multi-factor authentication protocol along with physical layer security techniques like destructively superimposed signal at the eavesdroppers and constructively superimposed signal at the receivers owing to beamforming at the zeRIS, on the contrary, will prevent an unauthorized access to the data of users. All these ethical developments combined together can ensure transparency and balance between confidential and safe communication in zeRIS-aided wireless networks.

1.4.2 Informed Judgments

Both software and hardware aspects of a zeRIS ought to be decided by the advice from experts in the field of new innovative wireless communication technologies working in the research and development department of regional companies or in higher educational institutions. Power allocation, superposition coding and user pairing based on the NOMA protocol, phase shift optimization, effective practical non-linear energy harvesting, installation of the zeRIS closer to access points or base stations and configuration of a operation mode for the zeRIS from available three modes like time-switching, mode selection or energy-splitting protocols will uphold technical aspects of the deployment of the technology. Both simulated and analytically obtained results for data rates of users in distinct settings, spectral and energy efficiency and outage probability would pave a way to assess both user-specific and overall system performances. As for awareness of decisions made during the project, getting a feedback from stakeholders, in particular from regional regulatory bodies, users and wireless service providers, would be valuable to ascertain that different parties are well-informed and get broader understanding of the societal implications of the project. Especially, a public consultation

with consumers helps to know whether they are content with the speed, fairness, security and smoothness of the newly introduced zeRIS-aided communication.

1.4.3 Global Context

It is expected that a zeRIS after proper testing and enhancement will find its application in developed countries in which 5G networks are beginning to work in urban areas, and then, in developing countries. A zeRIS is suited to regions even with limited operational cost like constrained power budget allocated to the zeRIS networks because it does not require supplementary power grid or battery to be charged and work regularly. Rather, it receives and harvests an energy from the incident RF signals, supporting an information transmission with a self-sustainability. Also, convenience of mounting a zeRIS in the walls of buildings due to absence of external power supplies makes zeRIS a good candidate for inexpensive energy efficient technology among other RISs or relays. The cost of the zeRIS is diminished by introducing an RF power combiner that feds to a single RF-to-DC conversion circuit of rectifier rather than having a rectifier per unit cell. Additionally, wireless communication via zeRIS is more affordable compared to wireline communication in which trenching and laying fiber optic cables is needed. This opportunity would attract attention of many developing countries as well as developed countries. To conclude, those features like self-sustainability, more realizable installation and budget-friendliness will facilitate a digital inclusion of all countries in spite of their economic situation.

1.4.4 Economic Impact

The early stages of deployment of the zeRIS require substantial amount of money for hardware acquisition, designing process and assessment of an environments that fit its installation. Nonetheless, these expenses can be defrayed by the high demand for 5GB services, both benefiting investors, telecom operators and users. Even if the implementation of the project may seem challenged for certain developing countries, the subsidies and grants from the government or international organizations could secure the realization of the task in some big cities of those regions, and then, widen it through a whole country gradually. Moreover, exploiting the same resource owing to NOMA saves the money for spectrum acquisition. In the long-term, zeRIS-aided NOMA networks will have a positive impact on e-commerce, fintech, and cloud-related services due to improved data rate and reliable communication. One of the significant advantages of the zeRIS is the energy efficiency. This will help to improve the communication where underdeveloped electricity infrastructure prevails. However, semi-autonomy of the zeRIS can cause in the reduction of some job places responsible for network management and maintenance. Meanwhile, there would be new unoccupied job places in a technology

sector dealing with zeRIS installation and energy harvesting that can compensate for the previous loss.

1.4.5 Environmental Impact

zeRIS is self-sustainable because of energy harvesting capability in addition to information transmission. Thus, using available RF signals in the air to harvest an energy at the same time with information delivery minimizes environmental harm by lowering a carbon footprint and greenhouse gas emissions caused by fossil-fueled energy generation. This important feature of zeRIS eliminates unnecessary air and noise pollution caused by constructions. NOMA power allocation and superposition coding diminishes a spectrum usage, and therefore, energy consumption because of reduced network traffic. Additionally, designing zeRIS elements with recyclable materials like biodegradable plastics and metals will mitigate accumulation of electronic wastes. zeRIS is particularly favorable in decreasing the reliance on base stations (BSs) per unit area because it provides alternative indirect path for the signal reception in the case when a direct link between a BS and receiver is blocked or suffer deep fading. Hence, land is free from additional BSs due to better coverage which is useful for protecting natural habitats and averting a deforestation and undesirable change of ecosystems within the urban natural and rural areas. Also, decreased number of BSs implies less electromagnetic pollution caused by emission of RF radiation that has been a dangerous resentment among opponents of 5G over the world.

1.4.6 Societal Impact

There would be new services available associated with development and maintenance of zeRIS, which will open new job opportunities for communication and technology specialists. Regarding wireless service providers, they would get improved data rate and coverage area which serve them as an innovative solution and opportunity for company growth. As for users, they would be provided with faster access to the Internet. Furthermore, the residents of remote or rural areas will get more access and comfortability to work from their home without relocating to the cities and metropolises. This will considerably prevent massive urban migration and support rural activity that became so scarce in recent centuries. Disabled or elder people who did not have a proper digital experience can receive telehealth services that assists in real-time healthcare consultations. Regarding students living in regions lacking a reliable internet access, the installation of zeRIS can enhance their engagement with online education platforms and provide a real-time access to live lectures given by internationally recognized professors. All of these factors contribute to speed up digital inclusion by narrowing the existing noticable gap between people living in populated cities and ordinary villages. As for public

safety and security, disaster-prone areas such as those subject to frequent earthquakes, hurricanes, floods and so on could be alerted about emergency quickly and without loss of connection.

Chapter 2

Methodology

This section elaborates network model, channel model, received signal model and energy consumption and harvesting models.

2.1 Network Model

This paper considers zeRIS-aided scheme in which a base station (BS) with a single antenna tries to communicate with single antenna user equipments at the reflection and transmission spaces, also known as UE_r and UE_t, respectively (see Fig. 2.1). There is a direct link between the BS and UE_r while a direct link between the BS and UE_t is blocked due to some environmental factors. The distances between the BS and zeRIS, zeRIS and UE_r, BS and UE_r and zeRIS and UE_t are denoted as d_{sz}, d_{zr}, d_{sr} and d_{zt}, respectively. It is assumed that the zeRIS operates under mode switching protocol. Let M be the number of metasurfaces of MF-RIS that have three modes of operation labeled as R mode, T mode and H mode for reflection, transmission/refraction and energy harvesting, respectively. Analogously, let M_r, M_t and M_h be the number of metasurfaces for those modes. Then, $M = M_r + M_t + M_h$. A reflection response matrix of zeRIS is denoted as $\mathbf{\Phi}_r = \beta_{\max}\text{diag}\left(\exp(\phi_r^{(1)}), \exp(\phi_r^{(2)}), \ldots, \exp(\phi_r^{(M_r)})\right)$ while a transmission response matrix of zeRIS is denoted as $\mathbf{\Phi}_t = \beta_{\max}\text{diag}\left(\exp(\phi_t^{(1)}), \exp(\phi_t^{(2)}), \ldots, \exp(\phi_t^{(M_t)})\right)$.

2.2 Channel Model

As we can see from Fig. 2.1, the channel between the BS and zeRIS as well as one between the zeRIS and UE_r and UE_t are denoted as $\mathbf{h}$, $\mathbf{g}_r$ and $\mathbf{g}_t$, respectively. The direct link between the base station and UE_r is labeled as h_d. Similarly, All channels are assumed to be independent Nakagami-m distributed flat fading channels. Furthermore, if the shape parameter $m_i = 1$ in which $i \in \{h, g_r, g_t, h_d\}$, the channel

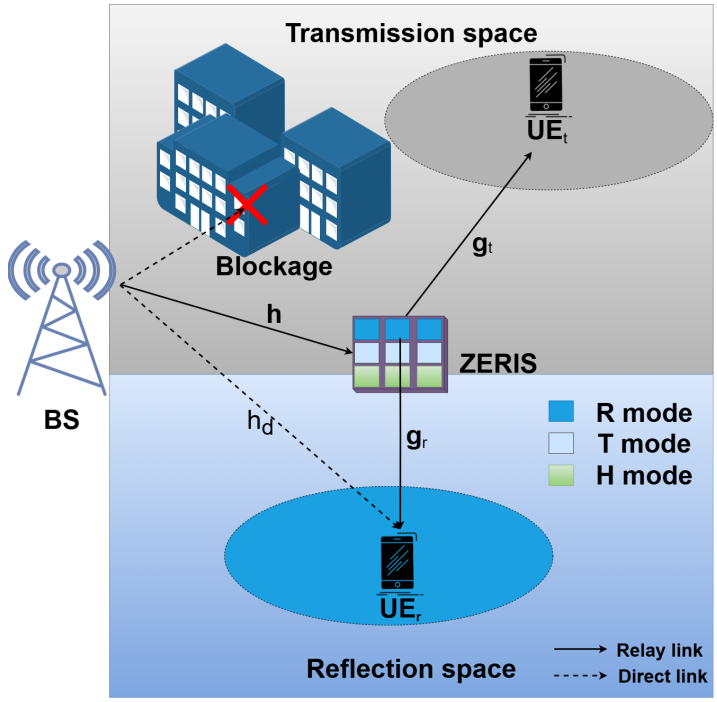

Figure 2.1: Proposed zeRIS-aided NOMA communication scheme.

would be a Rayleigh fading channel. As for $m_i > 1$, the channel would behave more as a Ricean fading channel. Channels incorporate a large-scale fading like 3GPP Urban Micro path loss given in [28]. Thus, a channel gain at a carrier frequency of 3 GHz is

$$\Omega_i(d)[\text{dB}] = \begin{cases} -37.5 - 22\log_{10}(d), & \text{if LoS,} \\ -35.1 - 36.7\log_{10}(d), & \text{if NLoS,} \end{cases} \tag{2.1}$$

where $i \in \{h, g_r, g_t, h_d\}$ and d is length of the link in meters.

2.3 Received Signal Model

According to NOMA protocol, a superimposed signal transmitted from the BS is

$$x = \sqrt{P}\left(\sqrt{\alpha_r}s_r + \sqrt{\alpha_t}s_t\right) \tag{2.2}$$

where power allocation coefficients α_r for UE$_r$ and α_t for UE$_t$ satisfy $\alpha_r + \alpha_t = 1$. $s_r \sim \mathcal{CN}(0,1)$ and $s_t \sim \mathcal{CN}(0,1)$ represent the desired symbols for UE$_r$ and UE$_t$, respectively. The received signal at UE$_r$ is

$$y_r = \left(\mathbf{g}_r^{\text{H}}\mathbf{\Phi}_r\mathbf{h}_r + d_r\right)x + \mathbf{g}_r^{\text{H}}\mathbf{\Phi}_r\mathbf{n}_r + n = \widehat{g}_r x + \mathbf{g}_r^{\text{H}}\mathbf{\Phi}_r\mathbf{n}_r + n, \tag{2.3}$$

where $\mathbf{n}_r \sim \mathcal{CN}\left(0, \sigma^2 \mathbf{I}_{M_r}\right)$ and $n \sim \mathcal{CN}\left(0, \sigma^2\right)$. The received signal at UE_t is

$$y_t = \mathbf{g}_t^{\mathrm{H}} \mathbf{\Phi}_t \mathbf{h}_t x + \mathbf{g}_t^{\mathrm{H}} \mathbf{\Phi}_t \mathbf{n}_t + n = \widehat{g}_t x + \mathbf{g}_t^{\mathrm{H}} \mathbf{\Phi}_t \mathbf{n}_t + n \tag{2.4}$$

where $\mathbf{n}_t \sim \mathcal{CN}\left(0, \sigma^2 \mathbf{I}_{M_t}\right)$. $\alpha_t > \alpha_r$ as long as UE_r is a strong user with better channel conditions while UE_t is regarded as a weak user. Therefore, direct decoding at UE_r gives a message of UE_t, and its signal-to-noise-plus-interference ratio (SINR) is

$$\gamma_{t \to r} = \frac{P \alpha_t \left|\widehat{g}_r\right|^2}{P \alpha_r \left|\widehat{g}_r\right|^2 + \left|\left|\mathbf{g}_r^{\mathrm{H}} \mathbf{\Phi}_r\right|\right|^2 \sigma^2 + \sigma^2} = \frac{\rho \alpha_t \mathcal{G}_r}{\rho \alpha_r \mathcal{G}_r + \left|\left|\mathbf{g}_r^{\mathrm{H}} \mathbf{\Phi}_r\right|\right|^2 + 1}, \tag{2.5}$$

where $\rho = \frac{P}{\sigma^2}$ and combined fading channel gain for UE_r is $\mathcal{G}_r = \left|\widehat{g}_r\right|^2$. After successive interference cancellation (SIC), UE_r decodes its own signal. The SNR is given by

$$\gamma_{r \to r} = \frac{P \alpha_r \left|\widehat{g}_r\right|^2}{\left|\left|\mathbf{g}_r^{\mathrm{H}} \mathbf{\Phi}_r\right|\right|^2 \sigma^2 + \sigma^2} = \frac{\rho \alpha_r \mathcal{G}_r}{\left|\left|\mathbf{g}_r^{\mathrm{H}} \mathbf{\Phi}_r\right|\right|^2 + 1}. \tag{2.6}$$

As for UE_t, it directly decodes its own signal while treating the signal of UE_r as an interference. It's SINR is

$$\gamma_{t \to t} = \frac{P \alpha_t \left|\widehat{g}_t\right|^2}{P \alpha_r \left|\widehat{g}_t\right|^2 + \left|\left|\mathbf{g}_t^{\mathrm{H}} \mathbf{\Phi}_t\right|\right|^2 \sigma^2 + \sigma^2} = \frac{\rho \alpha_t \mathcal{G}_t}{\rho \alpha_r \mathcal{G}_t + \left|\left|\mathbf{g}_t^{\mathrm{H}} \mathbf{\Phi}_t\right|\right|^2 + 1}, \tag{2.7}$$

where combined fading channel gain for UE_t is $\mathcal{G}_t = \left|\widehat{g}_t\right|^2$.

2.4 Energy Consumption and Harvesting Models

To achieve net zero energy at zeRIS, a new integrated architecture proposed in [29] is considered. Compared to traditional architectures in which a micro-controller such as Field Programmable Gate Arrays (FPGAs) are connected to the RIS unit cells through the drive circuits, integrated architecture includes chips that control impedance-adjusting semiconductors based on unit cell state. The integrated architecture can save a lot more power in comparison with micro-controller-based architectures. The total power consumed by zeRIS is

$$P_{\mathrm{RIS}} = P_{\mathrm{st}}^{\mathrm{tot}} + P_{\mathrm{dyn}}^{\mathrm{tot}}, \tag{2.8}$$

where $P_{\mathrm{st}}^{\mathrm{tot}}$ and $P_{\mathrm{dyn}}^{\mathrm{tot}}$ denote total static and dynamic power consumed by the ZERIS due to control chips and impedance-matching semiconductors, respectively. Assuming one control chip and one impedance-matching semiconductor per unit cell,

$$P_{\mathrm{st}}^{\mathrm{tot}} = M P_{\mathrm{st}}, \tag{2.9}$$

where P_{st} is a static power consumption per unit cell. As for dynamic power, it is

$$P_{\text{dyn}}^{\text{tot}} = (M_r + M_t)(P_b + P_{DC}) + P_C + \xi_{\text{RIS}} P_{\text{O}}, \tag{2.10}$$

where P_b, P_{DC} and P_C denote consumed power per phase shifter, by amplifier for DC biasing and by RF-to-DC power conversion circuit. ξ_{RIS} is the inverse amplifier efficiency of the RIS. The output power from zeRIS is given by

$$P_{\text{O}} = P\left(||\mathbf{\Phi}_r \mathbf{h}_r||^2 + ||\mathbf{\Phi}_t \mathbf{h}_t||^2\right) + \sigma^2 ||\mathbf{\Phi}_r||_{\text{F}}^2 + \sigma^2 ||\mathbf{\Phi}_t||_{\text{F}}^2, \tag{2.11}$$

because the reflected and transmitted signals from zeRIS are

$$\mathbf{y}_r^{\text{O}} = \mathbf{\Phi}_r(\mathbf{h}_r x + \mathbf{n}_r), \quad \mathbf{y}_t^{\text{O}} = \mathbf{\Phi}_t(\mathbf{h}_t x + \mathbf{n}_t). \tag{2.12}$$

Conversely, the incident signal on mth H mode cell is

$$y_{\text{RIS}}^m = h_h^m x + n_h, \tag{2.13}$$

where $n_h \sim \mathcal{CN}\left(0, \sigma^2\right)$. Leveraging RF power combiner, the total received RF power at zeRIS is

$$P_{\text{RF}}^{\text{tot}} = P \sum_{m=1}^{M_h} |h_h^{(m)}|^2, \tag{2.14}$$

in which a noise is omitted due to sensitivity of rectennas. Then, the total RF power is fed to a single rectifier to get a direct current (DC) power. The total harvested power assuming linear energy harvesting is

$$P_h^{\text{lin}} = \eta P_{\text{RF}}^{\text{tot}}, \tag{2.15}$$

where η is a energy conversion efficiency. Practically, energy harvesting behaves non-linearly relative to the number of energy harvesting elements. Based on [30],

$$\Omega = \frac{1}{1 + e^{ab}}, \quad \Psi = \frac{P_h^{\max}}{1 + e^{-a(P_{\text{RF}}^{\text{tot}} - b)}}, \tag{2.16}$$

$$P_h^{\text{non-lin}} = \frac{\Psi - P_h^{\max}\Omega}{1 - \Omega} = \frac{P_h^{\max}\left(\frac{1}{1+e^{-a(P_{\text{RF}}^{\text{tot}} - b)}} - \frac{1}{1+e^{ab}}\right)}{1 - \frac{1}{1+e^{ab}}}, \tag{2.17}$$

where Ω, a and b are constants that ensures zero input-zero output for energy harvesting and circuit specifications like resistance, capacity and diode turn-on voltage. Ψ is a logistic function with respect to a combined RF power by H mode elements of the zeRIS. $P_h^{\text{non-lin}}$ is the total power harvested by all H mode elements of the zeRIS. A critical amplification gain at the zeRIS is

$$\beta_{\max}^{\star} = \max\left(\frac{(P_h^{\text{type}} - MP_{\text{st}} - (M_r + M_t)(P_b + P_{DC}) - P_C)}{\xi_{\text{RIS}}(P(\sum_{m=1}^{M_r} |h_r^m|^2 + \sum_{m=1}^{M_t} |h_t^m|^2) + (M_r + M_t)\sigma^2)}, 0\right), \tag{2.18}$$

where type $= \{\text{lin}, \text{non} - \text{lin}\}$ indicates a type of energy harvesting model.

2.5 Performance analysis

Due to random nature of wireless communication, the ergodic rates were found to assess the performance of the system. The ergodic rate of UE_r is

$$R_r = \mathbb{E}\left[\log_2\left(1+\gamma_{r\to r}\right)\right] = \mathbb{E}\left[\log_2\left(1+\frac{P\alpha_t\mathcal{G}_r}{\sigma^2}\right)\right]. \tag{2.19}$$

The ergodic rate of UE_t is

$$R_t = \mathbb{E}\left[\log_2\left(1+\min(\gamma_{t\to r},\gamma_{t\to t})\right)\right], \tag{2.20}$$

where min ensures that both UEs can successfully decode the signal of UE_t.

A spectral efficiency is given by

$$SE = R_r + R_t, \tag{2.21}$$

whilst an energy efficiency is

$$EE = \frac{SE}{P_{\mathrm{tot}}} = \frac{SE}{\xi_s P + P_{\mathrm{BS}} + 2P_{\mathrm{U}}}, \tag{2.22}$$

where P_{tot} is the total power consumed by the network except zeRIS due to self-sustainability. ξ_s, P_{BS} and P_{U} are inverse amplifier efficiency at the BS, circuit power consumed by the BS and UE, respectively.

The outage probability at UE_r is

$$P_r^{\mathrm{out}} = \mathbb{P}\{R_r < R_r^{\mathrm{th}}\} = \mathbb{P}\{\gamma_{r\to r} < \gamma_r^{\mathrm{th}}\} = \mathbb{P}\left\{\frac{\rho\alpha_r\left|\widehat{g}_r\right|^2}{\left|\left|\mathbf{g}_r^{\mathrm{H}}\mathbf{\Phi}_r\right|\right|^2+1} < \gamma_r^{\mathrm{th}}\right\}, \tag{2.23}$$

where R_r^{th} and $\gamma_r^{\mathrm{th}} = 2^{R_r^{\mathrm{th}}} - 1$ are threshold data rate and SNR to successfully decode UE_r's signal, respectively. Similarly, the outage probability at UE_t is

$$\begin{aligned} P_t^{\mathrm{out}} &= \mathbb{P}\left\{R_t < R_t^{\mathrm{th}}\right\} = \mathbb{P}\left\{\min(\gamma_{t\to r},\gamma_{t\to t}) < \gamma_t^{\mathrm{th}}\right\} = 1 - \mathbb{P}\left\{\min(\gamma_{t\to r},\gamma_{t\to t})\right. \\ &\left.> \gamma_t^{\mathrm{th}}\right\} = 1 - \mathbb{P}\left\{\gamma_{t\to r} > \gamma_t^{\mathrm{th}}\right\} \times \mathbb{P}\left\{\gamma_{t\to t} > \gamma_t^{\mathrm{th}}\right\} = 1 - (1 - \mathbb{P}\left\{\gamma_{t\to r}\right. \\ &\left.< \gamma_t^{\mathrm{th}}\right\}) \times \left(1 - \mathbb{P}\left\{\gamma_{t\to t} < \gamma_t^{\mathrm{th}}\right\}\right) = \mathbb{P}\left\{\gamma_{t\to r} < \gamma_t^{\mathrm{th}}\right\} + \mathbb{P}\left\{\gamma_{t\to t} < \gamma_t^{\mathrm{th}}\right\} \\ &- \mathbb{P}\left\{\gamma_{t\to r} < \gamma_t^{\mathrm{th}}\right\} \times \mathbb{P}\left\{\gamma_{t\to t} < \gamma_t^{\mathrm{th}}\right\}, \end{aligned} \tag{2.24}$$

where R_t^{th} and $\gamma_t^{\mathrm{th}} = 2^{R_t^{\mathrm{th}}} - 1$ are threshold data rate and SINR to successfully decode UE_t's signal, respectively. The theoretical results of all metrics can found in Appendices A, B, C and D.

Chapter 3

Results and Discussions

The simulated results were obtained by Monte Carlo simulations in MATLAB with 100000 iterations. The simulation parameters are given in 3.1.

Table 3.1: Simulation Parameters

Parameter	**Value**
Power weight for UE_r	$\alpha_r = 0.2$
Noise Variance	$\sigma^2 = -70$ dBm
Threshold data rates	$R_r = 10$, $R_t = 2.31$
Distances	$\{d_{sz}, d_{zr}, d_{zt}, d_{sr}\} = \{10, 15, 10, 45\}$
Shape parameters	$\{m_{g_r}, m_{g_t}, m_h, m_{h_d}\} = \{2, 3, 5, 5\}$
Inverse amplifier efficiency at BS	$\xi_s = 1.1$
Inverse amplifier efficiency at zeRIS	$\xi_{\text{RIS}} = 1.1$
Power conversion efficiency	$\eta = 1$
Circuit specifications for non-linear energy harvesting	$a = 150$, $b = 0.014$
BS Circuit Power	$P_{\text{BS}} = 10$ dBm
Static power per unit cell	$P_{\text{st}} = 2\ \mu$W
Circuit Power at UEs	$P_{\text{U}} = 10$ dBm

3.1 Results

Firstly, we found amplification gains for different transmit powers at the BS for which net zero energy at the zeRIS is ensured (see **Figure 3.1**). Then, we considered a practical scenario in which zeRIS harvests energy according to non-linear

behavior. The performance metrics like ergodic rates, spectral and energy efficiencies and outage probability were plotted against transmit powers (see **Figure 3.2 - 3.5**).

The maximum amplification gain of zeRIS depends on how energy harvesting functions in the system. The non-linear EH model achieves a peak gain of 14 dB at -2 dBW transmit power which later decreases but the linear EH model demonstrates very rapid gain enhancement that reaches nearly 44 dB at power levels exceeding 8 dBW (see **Figure 3.1**).

UE_r's ergodic rate increases from 8 bits/s/Hz at -5 dBW transmit power to reach 14.5 bits/s/Hz at 20 dBW but UE_t maintains a fixed rate of about 2.5 bits/s/Hz during this power range as demonstrated in **Figure 3.2**.

The outage probability shows a reduction when transmit power elevates for all user equipments but UE_t demonstrates better outage performance compared to UE_r at every power setting (see Figure 3.3). The outage probability for UE_r follows 10^{-5} at a 20 dB transmit power but UE_t experiences a probability of roughly 0.01 as displayed in **Figure 3.3**.

The spectral efficiency rises with transmit power thus making it possible to achieve higher data rates as seen from **Figure 3.4**. The spectral efficiency evaluates at 10 bits/s/Hz when transmit power reaches -5 dB but achieves 17 bits/s/Hz at 20 dB (see **Figure 3.4**).

Energy efficiency experiences its highest decline when transmit power increases particularly during lower power settings as seen from **Figure 3.5**. The energy efficiency measurement decreases from 25 bits/Hz/J at -5 dB transmit power through 5 dB until reaching below 5 bits/Hz/J as shown in **Figure 3.5**.

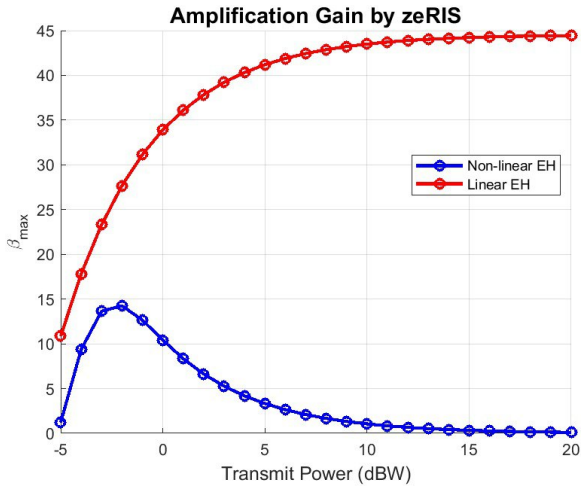

Figure 3.1: Amplification Gain of zeRIS for different energy harvesting models.

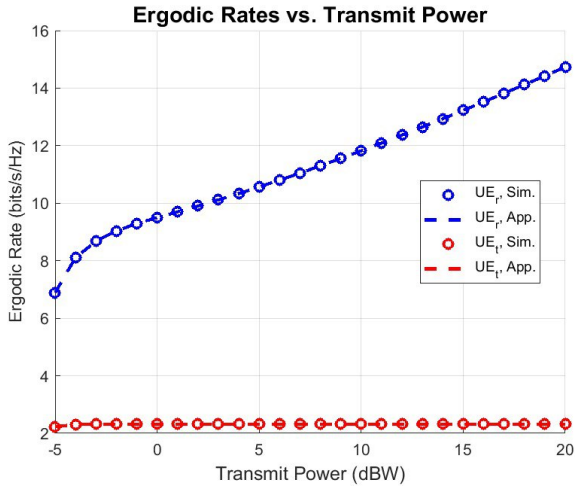

Figure 3.2: Ergodic Rates of UE$_r$ and UE$_r$ under self-sustainable operation of zeRIS and practical non-linear energy harvesting.

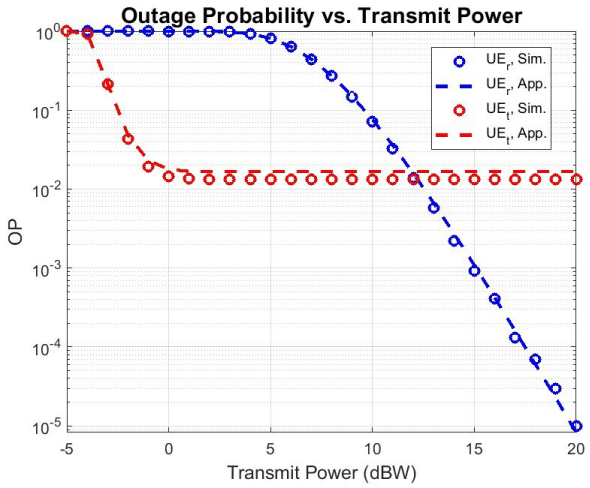

Figure 3.3: Outage probabilities for UE$_r$ and UE$_r$ under self-sustainable operation of zeRIS and practical non-linear energy harvesting.

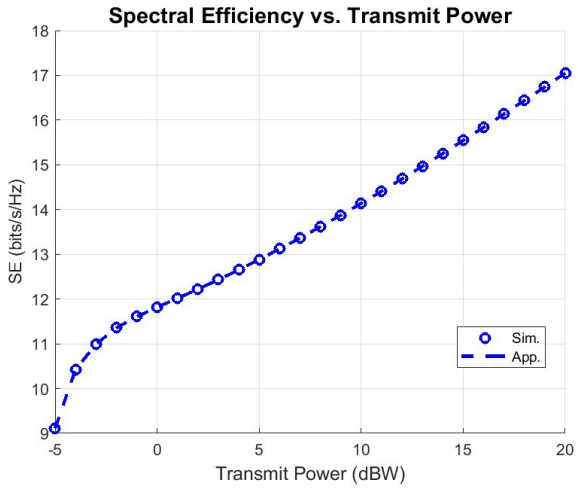

Figure 3.4: Spectral Efficiency under self-sustainable operation of zeRIS and practical non-linear energy harvesting.

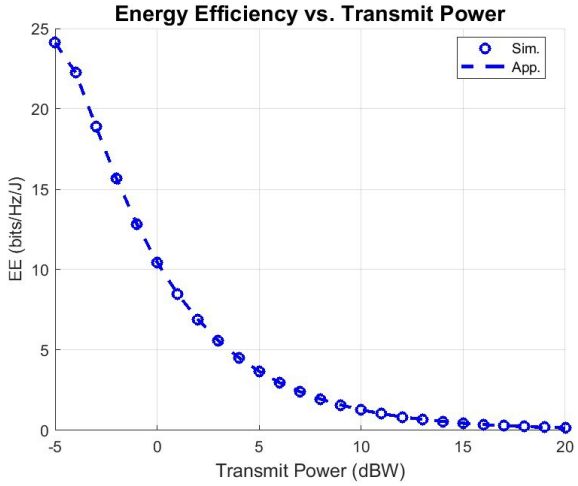

Figure 3.5: Energy Efficiency under self-sustainable operation of zeRIS and practical non-linear energy harvesting.

3.2 Discussion

Multiple key observations emerge from the study regarding the functioning of zeRIS systems. The direct relationship between energy efficiency and transmit power demonstrates that power boost can enhance spectral efficiency and reduce outages at the expense of energy consumption. The specified energy-efficiency trade-off becomes critical in situations that maintain limited energy availability. RIS-assisted user equipment location together with channel conditions determine how zeRIS systems perform by providing UE_r with better outage probability and ergodic rates than UE_t. User pairing strategies along with proper power allocation should be implemented to achieve fair and efficient wireless communication. The model selected for energy harvesting primarily determines the amplification strength of a zeRIS system. The peak gain behavior of non-linear power amplifiers indicates performance degradations may occur when transmit power is not properly optimized but the linear EH model delivers predictable performance levels with the increase in power. For zeRIS systems, the identification of proper transmit power stands as essential because it establishes the preferred levels of energy efficiency along with spectral efficiency and user fairness and outage probability. System performance would benefit from lower transmit power when energy efficiency requirements demand it even though spectral efficiency will decrease as a result. New research must develop power control methods which can automatically adjust power output according to changing channels together with shifting user positions. The assessment of enhanced energy harvesting techniques in connection with zeRIS performance demands greater investigation. The research needs to explore better strategies for minimizing differences between user performances through multi-user scheduling algorithms.

Chapter 4

Conclusion

The project evaluates zeRIS integration for NOMA systems through a design which enables RIS operation using ambient RF signal energy harvesting. Theoretical analysis and simulation demonstrate zeRIS's ability to waste less power along with improving broad system performance. The method provides a practical answer to create sustainable wireless communication networks.

Bibliography

[1] Yun Ai et al. "Secure Vehicular Communications Through Reconfigurable Intelligent Surfaces". In: *IEEE Transactions on Vehicular Technology* 70.7 (2021), pp. 7272–7276. DOI: 10.1109/TVT.2021.3088441.

[2] Marco Di Renzo, Fadil H. Danufane, and Sergei Tretyakov. "Communication Models for Reconfigurable Intelligent Surfaces: From Surface Electromagnetics to Wireless Networks Optimization". In: *Proceedings of the IEEE* 110.9 (2022), pp. 1164–1209. DOI: 10.1109/JPROC.2022.3195536.

[3] Junhui Rao et al. "A Novel Reconfigurable Intelligent Surface for Wide-Angle Passive Beamforming". In: *IEEE Transactions on Microwave Theory and Techniques* 70.12 (2022), pp. 5427–5439. DOI: 10.1109/TMTT.2022.3195224.

[4] Arman Shojaeifard et al. "MIMO Evolution Beyond 5G Through Reconfigurable Intelligent Surfaces and Fluid Antenna Systems". In: *Proceedings of the IEEE* 110.9 (2022), pp. 1244–1265. DOI: 10.1109/JPROC.2022.3170247.

[5] Ertugrul Basar et al. "Wireless Communications Through Reconfigurable Intelligent Surfaces". In: *IEEE Access* 7 (2019), pp. 116753–116773. DOI: 10.1109/ACCESS.2019.2935192.

[6] Yijin Pan et al. "Joint Deployment and Beamforming Design for STAR-RIS Aided Communication". In: *IEEE Communications Letters* 27.11 (2023), pp. 3083–3087. DOI: 10.1109/LCOMM.2023.3316620.

[7] Boqun Zhao et al. "Ergodic Rate Analysis of STAR-RIS Aided NOMA Systems". In: *IEEE Communications Letters* 26.10 (2022), pp. 2297–2301. DOI: 10.1109/LCOMM.2022.3194363.

[8] Jing Zhu et al. "Index Modulation for STAR-RIS Assisted NOMA System". In: *IEEE Communications Letters* 27.2 (2023), pp. 716–720. DOI: 10.1109/LCOMM.2022.3223968.

[9] Ruizhe Long et al. "Active Reconfigurable Intelligent Surface-Aided Wireless Communications". In: *IEEE Transactions on Wireless Communications* 20.8 (2021), pp. 4962–4975. DOI: 10.1109/TWC.2021.3064024.

[10] Zijian Zhang et al. "Active RIS vs. Passive RIS: Which Will Prevail in 6G?" In: *IEEE Transactions on Communications* 71.3 (2023), pp. 1707–1725. DOI: 10.1109/TCOMM.2022.3231893.

[11] Junhui Rao et al. "An Active Reconfigurable Intelligent Surface Utilizing Phase-Reconfigurable Reflection Amplifiers". In: *IEEE Transactions on Microwave Theory and Techniques* 71.7 (2023), pp. 3189–3202. DOI: 10.1109/TMTT.2023.3237029.

[12] Vatsala Sharma et al. "Robust Transmission for Energy-Efficient Sub-Connected Active RIS-Assisted Wireless Networks: DRL versus Traditional Optimization". In: *IEEE Transactions on Green Communications and Networking* (2024), pp. 1–1. DOI: 10.1109/TGCN.2024.3370691.

[13] Sravani Kurma et al. "Active RIS in Digital Twin-Based URLLC IoT Networks: Fully-Connected Versus Sub-Connected?" In: *IEEE Transactions on Wireless Communications* 23.9 (2024), pp. 12354–12367. DOI: 10.1109/TWC.2024.3391663.

[14] Kunzan Liu et al. "Active Reconfigurable Intelligent Surface: Fully-Connected or Sub-Connected?" In: *IEEE Communications Letters* 26.1 (2022), pp. 167–171. DOI: 10.1109/LCOMM.2021.3119696.

[15] Qi Zhu et al. "Joint Beamforming Designs for Active Reconfigurable Intelligent Surface: A Sub-Connected Array Architecture". In: *IEEE Transactions on Communications* 70.11 (2022), pp. 7628–7643. DOI: 10.1109/TCOMM.2022.3212749.

[16] Yajun Cheng, Wei Peng, and Tao Jiang. "Self-Sustainable RIS Aided Wireless Power Transfer Scheme". In: *IEEE Transactions on Vehicular Technology* 72.1 (2023), pp. 881–892. DOI: 10.1109/TVT.2022.3206086.

[17] Yijin Pan et al. "Self-Sustainable Reconfigurable Intelligent Surface Aided Simultaneous Terahertz Information and Power Transfer (STIPT)". In: *IEEE Transactions on Wireless Communications* 21.7 (2022), pp. 5420–5434. DOI: 10.1109/TWC.2022.3140268.

[18] Wen Wang et al. "Performance Analysis and Optimization of Reconfigurable Multi-Functional Surface Assisted Wireless Communications". In: *IEEE Transactions on Communications* 71.11 (2023), pp. 6695–6710. DOI: 10.1109/TCOMM.2023.3300333.

[19] Dimitrios Tyrovolas et al. "Comparing SWIPT Techniques for Zero-Energy RIS". In: *2023 IEEE International Conference on Communications Workshops (ICC Workshops)*. 2023, pp. 1848–1853. DOI: 10.1109/ICCWorkshops57953.2023.10283652.

[20] Dimitrios Tyrovolas et al. "Zero-Energy Reconfigurable Intelligent Surfaces (zeRIS)". In: *IEEE Transactions on Wireless Communications* 23.7 (2024), pp. 7013–7026. DOI: 10.1109/TWC.2023.3336956.

[21] Abdul Wahid et al. "Toward Secure and Scalable Vehicular Edge Computing With Zero-Energy RIS Using DRL". In: *IEEE Access* 12 (2024), pp. 129330–129346. DOI: 10.1109/ACCESS.2024.3457853.

[22] Yu Zheng et al. "Zero-Energy Device Networks With Wireless-Powered RISs". In: *IEEE Transactions on Vehicular Technology* 72.10 (2023), pp. 13655–13660. DOI: 10.1109/TVT.2023.3271874.

[23] Minsik Kim and Daeyoung Park. "Reconfigurable Intelligent Surfaces-Aided Federated Learning in Over-the-Air Computation". In: *IEEE Wireless Communications Letters* 13.7 (2024), pp. 1983–1987. DOI: 10.1109/LWC.2024.3399828.

[24] Muhammad Naqqash Tariq et al. "Toward Energy-Efficiency: Integrating DRL and Ze-RIS for Task Offloading in UAV-MEC Environments". In: *IEEE Access* 12 (2024), pp. 65530–65542. DOI: 10.1109/ACCESS.2024.3397890.

[25] Hakan Alakoca et al. "RIS-Empowered Non-Linear Energy Harvesting Communications Over Nakagami-m Channels". In: *IEEE Communications Letters* 26.9 (2022), pp. 2215–2219. DOI: 10.1109/LCOMM.2022.3182482.

[26] Shakil Ahmed et al. "Revolutionizing Batteryless IoT Systems to Enhance Nonlinear Energy Harvesting Using RIS Active and Passive Elements". In: *IEEE Open Journal of the Communications Society* 5 (2024), pp. 3021–3037. DOI: 10.1109/OJCOMS.2024.3393480.

[27] Mengqi Bian et al. "QoS-Aware Energy Storage Maximization in the RIS-Aided Joint-SWIPT-MEC System". In: *IEEE Communications Letters* 27.12 (2023), pp. 3434–3438. DOI: 10.1109/LCOMM.2023.3324716.

[28] Emil Björnson, Özgecan Özdogan, and Erik G. Larsson. "Intelligent Reflecting Surface Versus Decode-and-Forward: How Large Surfaces are Needed to Beat Relaying?" In: *IEEE Wireless Communications Letters* 9.2 (2020), pp. 244–248. DOI: 10.1109/LWC.2019.2950624.

[29] Konstantinos Ntontin et al. "Wireless Energy Harvesting for Autonomous Reconfigurable Intelligent Surfaces". In: *IEEE Transactions on Green Communications and Networking* 7.1 (2023), pp. 114–129. DOI: 10.1109/TGCN.2022.3201190.

[30] Elena Boshkovska et al. "Practical Non-Linear Energy Harvesting Model and Resource Allocation for SWIPT Systems". In: *IEEE Communications Letters* 19.12 (2015), pp. 2082–2085. DOI: 10.1109/LCOMM.2015.2478460.

Appendix A

Outage Probability of UE$_r$

$$P_r^{\text{out}} = \mathbb{P}\{\log_2(1+\gamma_{r\to r}) < R_r^{\text{th}}\} = \mathbb{P}\{\gamma_{r\to r} < \gamma_r^{\text{th}}\} = \mathbb{P}\left\{\frac{\rho\alpha_r |\widehat{g}_r|^2}{||\mathbf{g}_r^{\text{H}}\mathbf{\Phi}_r||^2 + 1} < \gamma_r^{\text{th}}\right\}$$
$$= \mathbb{P}\left\{\rho\alpha_r |\widehat{g}_r|^2 < \gamma_r^{\text{th}} \left|\left|\mathbf{g}_r^{\text{H}}\mathbf{\Phi}_r\right|\right|^2 + \gamma_r^{\text{th}}\right\} = \mathbb{P}\left\{\rho\alpha_r |\widehat{g}_r|^2 - \gamma_r^{\text{th}} \left|\left|\mathbf{g}_r^{\text{H}}\mathbf{\Phi}_r\right|\right|^2 < \gamma_r^{\text{th}}\right\}$$
$$= \mathbb{P}\left\{\frac{|\widehat{g}_r|^2}{\gamma_r^{\text{th}}} - \frac{||\mathbf{g}_r^{\text{H}}\mathbf{\Phi}_r||^2}{\rho\alpha_r} < \frac{1}{\rho\alpha_r}\right\} = \mathbb{P}\left\{\tilde{g}_r < \frac{1}{\rho\alpha_r}\right\}$$
$$= F_{\tilde{g}_r}(\frac{1}{\rho\alpha_r}) = \frac{\gamma(k_{\tilde{g}_r}, \frac{\frac{1}{\rho\alpha_r}}{\theta_{\tilde{g}_r}})}{\Gamma(k_{\tilde{g}_r})}, \quad \text{(A.1)}$$

where

$$k_{\tilde{g}_r} = \frac{\mathbb{E}[\tilde{g}_r]^2}{\mathbb{V}[\tilde{g}_r]}, \quad \theta_{\tilde{g}_r} = \frac{\mathbb{V}[\tilde{g}_r]}{\mathbb{E}[\tilde{g}_r]}. \quad \text{(A.2)}$$

According to **[nguyen2023performance]**, the pth moment of h_r^m, h_d, g_r^m and g_t^m are given as

$$\mu_{h_r}(p) \triangleq \frac{\Gamma(m_h + \frac{p}{2})}{\Gamma(m_h)} \left(\frac{\Omega_h}{m_h}\right)^{\frac{p}{2}}, \quad \text{(A.3)}$$

$$\mu_{h_d}(p) \triangleq \frac{\Gamma(m_{h_d} + \frac{p}{2})}{\Gamma(m_{h_d})} \left(\frac{\Omega_{h_d}}{m_{h_d}}\right)^{\frac{p}{2}}, \quad \text{(A.4)}$$

$$\mu_{g_r}(p) \triangleq \frac{\Gamma(m_{g_r} + \frac{p}{2})}{\Gamma(m_{g_r})} \left(\frac{\Omega_{g_r}}{m_{g_r}}\right)^{\frac{p}{2}}, \quad \text{(A.5)}$$

$$\mu_{g_t}(p) \triangleq \frac{\Gamma(m_{g_t} + \frac{p}{2})}{\Gamma(m_{g_t})} \left(\frac{\Omega_{g_t}}{m_{g_t}}\right)^{\frac{p}{2}}. \quad \text{(A.6)}$$

Obviously, $\mu_{h_t}(p) = \mu_{h_h}(p) = \mu_{h_r}(p)$. Now,

$$\mathbb{E}\left[\tilde{g}_r\right] = \mathbb{E}\left[\frac{\left(\sqrt{\beta_{max}}\sum_{m=1}^{M_r}\left(|g_r^{(m)}||h_r^{(m)}|\right)+|h_d|\right)^2}{\gamma_r^{\text{th}}} - \frac{\beta_{\max}\sum_{m=1}^{M_r}|g_r^{(m)}|^2}{\rho\alpha_r}\right]$$

$$= \frac{1}{\gamma_r^{\text{th}}}\mathbb{E}\left[\left(\sqrt{\beta_{max}}\sum_{m=1}^{M_r}\left(|g_r^{(m)}||h_r^{(m)}|\right)+|h_d|\right)^2\right] - \frac{\beta_{\max}}{\rho\alpha_r}\mathbb{E}\left[\sum_{m=1}^{M_r}|g_r^{(m)}|^2\right]$$

$$= \frac{1}{\gamma_r^{\text{th}}}\Bigg(\beta_{max}\underbrace{\mathbb{E}\left[\left(\sum_{m=1}^{M_r}|g_r^{(m)}||h_r^{(m)}|\right)^2\right]}_{A_r} + 2\sqrt{\beta_{max}}\mathbb{E}\left[|h_d|\right]\underbrace{\mathbb{E}\left[\sum_{m=1}^{M_r}\left(|g_r^{(m)}||h_r^{(m)}|\right)\right]}_{B_r}$$

$$+\mathbb{E}\left[|h_d|^2\right]\Bigg) - \frac{\beta_{\max}}{\rho\alpha_r}\sum_{m=1}^{M_r}\mathbb{E}\left[|g_r^{(m)}|^2\right] = \frac{1}{\gamma_r^{\text{th}}}\Big(\beta_{\max}M_r\Omega_{g_r}\Omega_h$$

$$+\beta_{\max}M_r(M_r-1)\left(\frac{\Gamma(m_{g_r}+\frac{1}{2})}{\Gamma(m_{g_r})}\right)^2\left(\frac{\Omega_{g_r}}{m_{g_r}}\right)\left(\frac{\Gamma(m_h+\frac{1}{2})}{\Gamma(m_h)}\right)^2\left(\frac{\Omega_h}{m_h}\right)$$

$$+2\sqrt{\beta_{\max}}M_r\frac{\Gamma(m_{g_r}+\frac{1}{2})}{\Gamma(m_{g_r})}\left(\frac{\Omega_{g_r}}{m_{g_r}}\right)^{\frac{1}{2}}\frac{\Gamma(m_h+\frac{1}{2})}{\Gamma(m_h)}\left(\frac{\Omega_h}{m_h}\right)^{\frac{1}{2}}\frac{\Gamma(m_{h_d}+\frac{1}{2})}{\Gamma(m_{h_d})}\left(\frac{\Omega_{h_d}}{m_{h_d}}\right)^{\frac{1}{2}}+\Omega_{h_d}\Big)$$

$$-\frac{\beta_{\max}M_r\Omega_{g_r}}{\rho\alpha_r}, \quad \text{(A.7)}$$

where

$$A_r = \mathbb{E}\left[\left(\sum_{m=1}^{M_r}|g_r^{(m)}||h_r^{(m)}|\right)^2\right]$$

$$= \mathbb{E}\left[\sum_{m=1}^{M_r}\left(|g_r^{(m)}|^2|h_r^{(m)}|^2\right)+\sum_{1\le i\ne j\le M_r}|g_r^{(i)}||h_r^{(i)}||g_r^{(j)}||h_r^{(j)}|\right]$$

$$= \sum_{m=1}^{M_r}\mathbb{E}\left[|g_r^{(m)}|^2\right]\mathbb{E}\left[|h_r^{(m)}|^2\right]+\sum_{1\le i\ne j\le M_r}\mathbb{E}\left[|g_r^{(i)}|\right]\mathbb{E}\left[|g_r^{(j)}|\right]\mathbb{E}\left[|h_r^{(i)}|\right]\mathbb{E}\left[|h_r^{(j)}|\right]$$

$$= M_r\Omega_{g_r}\Omega_h + M_r(M_r-1)\left(\frac{\Gamma(m_{g_r}+\frac{1}{2})}{\Gamma(m_{g_r})}\right)^2\left(\frac{\Omega_{g_r}}{m_{g_r}}\right)\left(\frac{\Gamma(m_h+\frac{1}{2})}{\Gamma(m_h)}\right)^2\left(\frac{\Omega_h}{m_h}\right) \quad \text{(A.8)}$$

and

$$B_r = \mathbb{E}\left[\sum_{m=1}^{M_r}\left(|g_r^{(m)}||h_r^{(m)}|\right)\right] = \mathbb{E}\left[\sum_{m=1}^{M_r}\left(|g_r^{(m)}||h_r^{(m)}|\right)\right]$$
$$= \sum_{m=1}^{M_r}\mathbb{E}\left[|g_r^{(m)}|\right]\mathbb{E}\left[|h_r^{(m)}|\right] = M_r\frac{\Gamma(m_{g_r}+\frac{1}{2})}{\Gamma(m_{g_r})}\left(\frac{\Omega_{g_r}}{m_{g_r}}\right)^{\frac{1}{2}}\frac{\Gamma(m_h+\frac{1}{2})}{\Gamma(m_h)}\left(\frac{\Omega_h}{m_h}\right)^{\frac{1}{2}}. \quad \text{(A.9)}$$

Then,

$$\mathbb{E}\left[\tilde{g}_r^2\right] = \frac{1}{(\gamma_r^{\text{th}})^2}\Bigg(\beta_{\max}^2\underbrace{\mathbb{E}\left[\left(\sum_{m=1}^{M_r}|g_r^{(m)}||h_r^{(m)}|\right)^4\right]}_{C_r} + 4\beta_{\max}^{\frac{3}{2}}$$
$$\times\,\mathbb{E}\left[|h_d|\right]\underbrace{\mathbb{E}\left[\left(\sum_{m=1}^{M_r}|g_r^{(m)}||h_r^{(m)}|\right)^3\right]}_{D_r} + 6\beta_{\max}\mathbb{E}\left[|h_d|^2\right]$$
$$\times\,\underbrace{\mathbb{E}\left[\left(\sum_{m=1}^{M_r}|g_r^{(m)}||h_r^{(m)}|\right)^2\right]}_{A_r} + 4\sqrt{\beta_{\max}}\mathbb{E}\left[|h_d|^3\right]$$
$$\times\,\underbrace{\mathbb{E}\left[\left(\sum_{m=1}^{M_r}|g_r^{(m)}||h_r^{(m)}|\right)\right]}_{B_r} + \mathbb{E}\left[|h_d|^4\right]\Bigg) - \frac{2\beta_{\max}}{\gamma_r^{\text{th}}\rho\alpha_r}\left(\beta_{\max}\right.$$
$$\times\,\underbrace{\mathbb{E}\left[\left(\sum_{m=1}^{M_r}|g_r^{(m)}||h_r^{(m)}|\right)^2\sum_{m=1}^{M_r}|g_r^{(m)}|^2\right]}_{E_r} + 2\sqrt{\beta_{\max}}$$
$$\times\,\mathbb{E}\left[|h_d|\right]\underbrace{\mathbb{E}\left[\left(\sum_{m=1}^{M_r}|g_r^{(m)}||h_r^{(m)}|\right)\sum_{m=1}^{M_r}|g_r^{(m)}|^2\right]}_{F_r} + \mathbb{E}\left[|h_d|^2\right]$$
$$\left.\times\sum_{m=1}^{M_r}\mathbb{E}\left[|g_r^{(m)}|^2\right]\right) + \frac{\beta_{\max}^2}{(\rho\alpha_r)^2}\underbrace{\mathbb{E}\left[\left(\sum_{m=1}^{M_r}|g_r^{(m)}|^2\right)^2\right]}_{H_r}, \quad \text{(A.10)}$$

Let us denote $\mathcal{K}$ as $\{k_1, k_2, \ldots, k_{M_r}\}$. Then,

$$
\begin{aligned}
C_r = \mathbb{E}\left[\left(\sum_{m=1}^{M_r} |g_r^{(m)}||h_r^{(m)}|\right)^4\right] &= \mathbb{E}\left[\sum_{k_1+k_2+\cdots+k_{M_r}=4} 4!\right. \\
&\times \frac{1}{k_1!k_2!\ldots k_{M_r}!}\left(|g_r^{(1)}||h_r^{(1)}|\right)^{k_1}\left(|g_r^{(2)}||h_r^{(2)}|\right)^{k_2} \\
&\left.\ldots\left(|g_r^{(M_r)}||h_r^{(M_r)}|\right)^{k_{M_r}}\right] = \mathbb{E}\left[\sum_{\mathcal{K}=\{4,0,0,\ldots,0\},\ 1\le i\le M_r} \frac{4!}{4!}\right. \\
&\times\left(|g_r^{(i)}||h_r^{(i)}|\right)^4 + \sum_{\mathcal{K}=\{3,1,0,\ldots,0\},\ 1\le i\ne j\le M_r} \frac{4!}{3!} \\
&\times\left(|g_r^{(i)}||h_r^{(i)}|\right)^3\left(|g_r^{(j)}||h_r^{(j)}|\right) \\
&+ \sum_{\mathcal{K}=\{2,2,0,\ldots,0\},\ 1\le i\ne j\le M_r} \frac{4!}{2!2!}\left(|g_r^{(i)}||h_r^{(i)}|\right)^2 \\
&\times\left(|g_r^{(j)}||h_r^{(j)}|\right)^2 + \sum_{\mathcal{K}=\{2,1,1,0,\ldots,0\},\ 1\le i\ne j\ne l\le M_r} \frac{4!}{2!} \\
&\times\left(|g_r^{(i)}||h_r^{(i)}|\right)^2\left(|g_r^{(j)}||h_r^{(j)}|\right)\left(|g_r^{(l)}||h_r^{(l)}|\right) \\
&+ \sum_{\mathcal{K}=\{1,1,1,1,0,\ldots,0\},\ 1\le i\ne j\ne l\ne n\le M_r} \frac{4!}{1!}\left(|g_r^{(i)}||h_r^{(i)}|\right) \\
&\times\left(|g_r^{(j)}||h_r^{(j)}|\right)\left(|g_r^{(l)}||h_r^{(l)}|\right)\left(|g_r^{(n)}||h_r^{(n)}|\right) \\
&= \sum_{\mathcal{K}=\{4,0,0,\ldots,0\},\ 1\le i\le M_r} \frac{4!}{4!}\mathbb{E}\left[|g_r^{(i)}|^4\right]\mathbb{E}\left[|h_r^{(i)}|^4\right] \\
&+ \sum_{\mathcal{K}=\{3,1,0,\ldots,0\},\ 1\le i\ne j\le M_r} \frac{4!}{3!}\mathbb{E}\left[|g_r^{(i)}|^3\right]\mathbb{E}\left[|h_r^{(i)}|^3\right] \\
&\times\mathbb{E}\left[|g_r^{(j)}|\right]\mathbb{E}\left[|h_r^{(j)}|\right] + \sum_{\mathcal{K}=\{2,2,0,\ldots,0\},\ 1\le i\ne j\le M_r} \frac{4!}{2!2!} \\
&\times\mathbb{E}\left[|g_r^{(i)}|^2\right]\mathbb{E}\left[|h_r^{(i)}|^2\right]\mathbb{E}\left[|g_r^{(j)}|^2\right]\mathbb{E}\left[|h_r^{(j)}|^2\right] \\
&+ \sum_{\mathcal{K}=\{2,1,1,0,\ldots,0\},\ 1\le i\ne j\ne l\le M_r} \frac{4!}{2!}\mathbb{E}\left[|g_r^{(i)}|^2\right]\mathbb{E}\left[|h_r^{(i)}|^2\right] \\
&\times\mathbb{E}\left[|g_r^{(j)}|\right]\mathbb{E}\left[|h_r^{(j)}|\right]\mathbb{E}\left[|g_r^{(l)}|\right]\mathbb{E}\left[|h_r^{(l)}|\right] \\
&+ \sum_{\mathcal{K}=\{1,1,1,1,0,\ldots,0\},\ 1\le i\ne j\ne l\ne n\le M_r} \frac{4!}{1!}\mathbb{E}\left[|g_r^{(i)}|\right]\mathbb{E}\left[|h_r^{(i)}|\right] \\
&\times\mathbb{E}\left[|g_r^{(j)}|\right]\mathbb{E}\left[|h_r^{(j)}|\right]\mathbb{E}\left[|g_r^{(l)}|\right]\mathbb{E}\left[|h_r^{(l)}|\right]\mathbb{E}\left[|g_r^{(n)}|\right]\mathbb{E}\left[|h_r^{(n)}|\right], \quad \text{(A.11)}
\end{aligned}
$$

which is

$$
\begin{aligned}
C_r = \frac{4!}{4!} M_r m_{g_r}(m_{g_r}+1)\left(\frac{\Omega_{g_r}}{m_{g_r}}\right)^2 m_h(m_h+1)\left(\frac{\Omega_h}{m_h}\right)^2 \\
+ \frac{4!}{3!}\frac{M_r(M_r-1)}{2!}\frac{\Gamma(m_{g_r}+\frac{3}{2})}{\Gamma(m_{g_r})}\left(\frac{\Omega_{g_r}}{m_{g_r}}\right)^2 \frac{\Gamma(m_h+\frac{3}{2})}{\Gamma(m_h)} \\
\times \left(\frac{\Omega_h}{m_h}\right)^2 \left(\frac{\Gamma(m_{g_r}+\frac{1}{2})}{\Gamma(m_{g_r})}\right)\left(\frac{\Gamma(m_h+\frac{1}{2})}{\Gamma(m_h)}\right) + \frac{4!}{2!2!} \\
\times \frac{M_r(M_r-1)}{2!}\Omega_{g_r}^2\Omega_h^2 + \frac{4}{2!}\frac{M_r(M_r-1)(M_r-2)}{3!} \\
\times \frac{\Omega_{g_r}^2}{m_{g_r}}\frac{\Omega_h^2}{m_h}\left(\frac{\Gamma(m_{g_r}+\frac{1}{2})}{\Gamma(m_{g_r})}\right)^2\left(\frac{\Gamma(m_h+\frac{1}{2})}{\Gamma(m_h)}\right)^2 + \frac{4!}{1!} \\
\times \frac{M_r(M_r-1)(M_r-2)(M_r-3)}{4!}\left(\frac{\Omega_{g_r}}{m_{g_r}}\right)^2\left(\frac{\Omega_h}{m_h}\right)^2 \\
\times \left(\frac{\Gamma(m_{g_r}+\frac{1}{2})}{\Gamma(m_{g_r})}\right)^4\left(\frac{\Gamma(m_h+\frac{1}{2})}{\Gamma(m_h)}\right)^4 . \qquad \text{(A.12)}
\end{aligned}
$$

$$D_r = \mathbb{E}\left[\left(\sum_{m=1}^{M_r} |g_r^{(m)}||h_r^{(m)}|\right)^3\right] = \mathbb{E}\left[\sum_{k_1+k_2+\cdots+k_{M_r}=3} 3! \times \frac{1}{k_1!k_2!\ldots k_{M_r}!}\left(|g_r^{(m)}||h_r^{(m)}|\right)^{k_1}\left(|g_r^{(m)}||h_r^{(m)}|\right)^{k_2} \ldots \left(|g_r^{(m)}||h_r^{(m)}|\right)^{k_{M_r}}\right] = \mathbb{E}\left[\sum_{\mathcal{K}=\{3,0,0,\ldots,0\},\ 1\le i\le M_r} \frac{3!}{3!} \times \left(|g_r^{(i)}||h_r^{(i)}|\right)^3 + \sum_{\mathcal{K}=\{2,1,0,\ldots,0\},\ 1\le i\ne j\le M_r} \frac{3!}{2!} \times \left(|g_r^{(i)}||h_r^{(i)}|\right)^2\left(|g_r^{(j)}||h_r^{(j)}|\right) + \sum_{\mathcal{K}=\{1,1,1,0,\ldots,0\},\ 1\le i\ne j\ne l\le M_r} \frac{3!}{1!}\left(|g_r^{(i)}||h_r^{(i)}|\right) \times \left(|g_r^{(j)}||h_r^{(j)}|\right)\left(|g_r^{(l)}||h_r^{(l)}|\right)\right] = \sum_{\mathcal{K}=\{3,0,0,\ldots,0\},\ 1\le i\le M_r} \frac{3!}{3!} \times \mathbb{E}\left[|g_r^{(i)}|^3\right]\mathbb{E}\left[|h_r^{(i)}|^3\right] + \sum_{\mathcal{K}=\{2,1,0,\ldots,0\},\ 1\le i\ne j\le M_r} \frac{3!}{2!} \times \mathbb{E}\left[\left(|g_r^{(i)}||h_r^{(i)}|\right)^2\left(|g_r^{(j)}||h_r^{(j)}|\right)\right] + \sum_{\mathcal{K}=\{1,1,1,0,\ldots,0\},\ 1\le i\ne j\ne l\le M_r} \frac{3!}{1!}\mathbb{E}\left[|g_r^{(i)}|\right]\mathbb{E}\left[|h_r^{(i)}|\right] \times \mathbb{E}\left[|g_r^{(j)}|\right]\mathbb{E}\left[|h_r^{(j)}|\right]\mathbb{E}\left[|g_r^{(l)}|\right]\mathbb{E}\left[|h_r^{(l)}|\right], \quad \text{(A.13)}$$

which is

$$D_r = \frac{3!}{3!}M_r\frac{\Gamma(m_{g_r}+\frac{3!}{2})}{\Gamma(m_{g_r})}\left(\frac{\Omega_{g_r}}{m_{g_r}}\right)^{\frac{3}{2}}\frac{\Gamma(m_h+\frac{3}{2})}{\Gamma(m_h)}\left(\frac{\Omega_h}{m_h}\right)^{\frac{3}{2}} + \frac{3!}{2!}\frac{M_r(M_r-1)}{2!}\Omega_{g_r}\Omega_h\frac{\Gamma(m_{g_r}+\frac{1}{2})}{\Gamma(m_{g_r})}\left(\frac{\Omega_{g_r}}{m_{g_r}}\right)^{\frac{1}{2}} \times \frac{\Gamma(m_h+\frac{1}{2})}{\Gamma(m_h)}\left(\frac{\Omega_h}{m_h}\right)^{\frac{1}{2}} + \frac{3!}{1!}\frac{M_r(M_r-1)(M_r-2)}{3!} \times \left(\frac{\Gamma(m_{g_r}+\frac{1}{2})}{\Gamma(m_{g_r})}\right)^3\left(\frac{\Omega_{g_r}}{m_{g_r}}\right)^{\frac{3}{2}}\left(\frac{\Gamma(m_h+\frac{1}{2})}{\Gamma(m_h)}\right)^3\left(\frac{\Omega_h}{m_h}\right)^{\frac{3}{2}} \quad \text{(A.14)}$$

$$E_r = \mathbb{E}\left[\left(\sum_{m=1}^{M_r}|g_r^{(m)}||h_r^{(m)}|\right)^2\sum_{m=1}^{M_r}|g_r^{(m)}|^2\right]$$
$$= \mathbb{E}\left[\left(\sum_{m=1}^{M_r}\left(|g_r^{(m)}|^2|h_r^{(m)}|^2\right)+\sum_{1\le i\ne j\le M_r}|g_r^{(i)}||h_r^{(i)}|\right.\right.$$
$$\left.\left.\times|g_r^{(j)}||h_r^{(j)}|\right)\sum_{m=1}^{M_r}|g_r^{(m)}|^2\right] = \mathbb{E}\left[\sum_{m=1}^{M_r}\left(|g_r^{(m)}|^4|h_r^{(m)}|^2\right)\right.$$
$$+\sum_{1\le i\ne j\le M_r}\left(|g_r^{(i)}|^2|g_r^{(j)}|^2|h_r^{(i)}|^2\right)+\sum_{1\le i\ne j\le M_r}|g_r^{(i)}|^3$$
$$\times|h_r^{(i)}||g_r^{(j)}||h_r^{(j)}|+\sum_{1\le i\ne j\le M_r}|g_r^{(i)}||h_r^{(i)}||g_r^{(j)}|^3|h_r^{(j)}|$$
$$\left.+\sum_{i\ne j\ne l}|g_r^{(i)}||h_r^{(i)}||g_r^{(j)}||h_r^{(j)}||g_r^{(l)}|^2\right] = \sum_{m=1}^{M_r}\mathbb{E}\left[|g_r^{(m)}|^4\right]$$
$$\times\mathbb{E}\left[|h_r^{(m)}|^2\right]+\sum_{1\le i\ne j\le M_r}\mathbb{E}\left[|g_r^{(i)}|^2\right]\mathbb{E}\left[|g_r^{(j)}|^2\right]$$
$$\times\mathbb{E}\left[|h_r^{(i)}|^2\right]+\sum_{1\le i\ne j\le M_r}\mathbb{E}\left[|g_r^{(i)}|^3\right]\mathbb{E}\left[|h_r^{(i)}|\right]\mathbb{E}\left[|g_r^{(j)}|\right]$$
$$\times\mathbb{E}\left[|h_r^{(j)}|\right]+\sum_{1\le i\ne j\le M_r}\mathbb{E}\left[|g_r^{(i)}|^3\right]\mathbb{E}\left[|h_r^{(i)}|\right]\mathbb{E}\left[|g_r^{(j)}|^3\right]$$
$$\times\mathbb{E}\left[|h_r^{(j)}|\right]+\sum_{i\ne j\ne l}\mathbb{E}\left[|g_r^{(i)}||h_r^{(i)}||g_r^{(j)}||h_r^{(j)}||g_r^{(l)}|^2\right], \quad \text{(A.15)}$$

which is

$$E_r = M_r m_{g_r}(m_{g_r}+1)\left(\frac{\Omega_{g_r}}{m_{g_r}}\right)^2\Omega_h + M_r(M_r-1)\Omega_{g_r}^2\Omega_h$$
$$+2M_r(M_r-1)\frac{\Gamma(m_{g_r}+\frac{3}{2})}{\Gamma(m_{g_r})}\left(\frac{\Omega_{g_r}}{m_{g_r}}\right)^2\frac{\Gamma(m_{g_r}+\frac{1}{2})}{\Gamma(m_{g_r})}$$
$$\times\left(\frac{\Gamma(m_h+\frac{1}{2})}{\Gamma(m_h)}\right)^2\left(\frac{\Omega_h}{m_h}\right)+\frac{M_r(M_r-1)(M_r-2)}{3!}$$
$$\times\frac{\Omega_{g_r}^2}{m_{g_r}}\frac{\Omega_h}{m_h}\left(\frac{\Gamma(m_{g_r}+\frac{1}{2})}{\Gamma(m_{g_r})}\right)^2\left(\frac{\Gamma(m_h+\frac{1}{2})}{\Gamma(m_h)}\right)^2. \quad \text{(A.16)}$$

$$F_r = \mathbb{E}\left[\left(\sum_{m=1}^{M_r} |g_r^{(m)}||h_r^{(m)}|\right)\sum_{m=1}^{M_r}|g_r^{(m)}|^2\right]$$
$$= \mathbb{E}\left[\sum_{m=1}^{M_r}|g_r^{(m)}|^3|h_r^{(m)}| + \sum_{1\le i\neq j\le M_r}|g_r^{(i)}||g_r^{(j)}|^2|h_r^{(i)}|\right]$$
$$= \sum_{m=1}^{M_r}\mathbb{E}\left[|g_r^{(m)}|^3\right]\mathbb{E}\left[|h_r^{(m)}|\right] + \sum_{1\le i\neq j\le M_r}\mathbb{E}\left[|g_r^{(i)}|\right]$$
$$\times\,\mathbb{E}\left[|g_r^{(j)}|^2\right]\mathbb{E}\left[|h_r^{(i)}|\right] = M_r\frac{\Gamma(m_{g_r}+\frac{3}{2})}{\Gamma(m_{g_r})}\left(\frac{\Omega_{g_r}}{m_{g_r}}\right)^{\frac{3}{2}}$$
$$\times\,\frac{\Gamma(m_{h_r}+\frac{1}{2})}{\Gamma(m_{h_r})}\left(\frac{\Omega_h}{m_h}\right)^{\frac{1}{2}} + M_r(M_r-1)\Omega_{g_r}\frac{\Gamma(m_{g_r}+\frac{1}{2})}{\Gamma(m_{g_r})}$$
$$\times\left(\frac{\Omega_{g_r}}{m_{g_r}}\right)^{\frac{1}{2}}\frac{\Gamma(m_h+\frac{1}{2})}{\Gamma(m_h)}\left(\frac{\Omega_h}{m_h}\right)^{\frac{1}{2}}. \quad \text{(A.17)}$$

$$H_r = \mathbb{E}\left[\left(\sum_{m=1}^{M_r}|g_r^{(m)}|^2\right)^2\right] = \mathbb{E}\left[\sum_{m=1}^{M_r}|g_r^{(m)}|^4\right.$$
$$\left. + \sum_{1\le i\neq j\le M_r}|g_r^{(i)}|^2|g_r^{(j)}|^2\right] = \sum_{m=1}^{M_r}\mathbb{E}\left[|g_r^{(m)}|^4\right]$$
$$+ \sum_{1\le i\neq j\le M_r}\mathbb{E}\left[|g_r^{(i)}|^2\right]\mathbb{E}\left[|g_r^{(j)}|^2\right]$$
$$= M_r m_{g_r}(m_{g_r}+1)\left(\frac{\Omega_{g_r}}{m_{g_r}}\right)^2 + M_r(M_r-1)\Omega_{g_r}^2. \quad \text{(A.18)}$$

Afterwards, the variance can be find as

$$\mathbb{V}\left[\tilde{g}_r\right] = \mathbb{E}\left[\tilde{g}_r^2\right] - \left(\mathbb{E}\left[\tilde{g}_r\right]\right)^2, \quad \text{(A.19)}$$

and we get $k_{\tilde{g}_r}$ and $\theta_{\tilde{g}_r}$ defined in (A.2). Also,

$$I_r = \mathbb{E}\left[\mathcal{G}_r\right] = \beta_{\max}A_r + 2\sqrt{\beta_{\max}}\frac{\Gamma(m_{h_d}+\frac{1}{2})}{\Gamma(m_{h_d})}\left(\frac{\Omega_{h_d}}{m_{h_d}}\right)^{\frac{1}{2}}B_r + \Omega_{h_d}, \quad \text{(A.20)}$$

and

$$J_r = \mathbb{E}\left[\mathcal{G}_r^2\right] = \beta_{\max}^2 C_r + 4\beta_{\max}^{\frac{3}{2}}\frac{\Gamma(m_{h_d}+\frac{1}{2})}{\Gamma(m_{h_d})}\left(\frac{\Omega_{h_d}}{m_{h_d}}\right)^{\frac{1}{2}}D_r$$
$$+ 6\beta_{\max}\Omega_{h_d}E_r + 4\beta_{\max}^{\frac{1}{2}}\frac{\Gamma(m_{h_d}+\frac{3}{2})}{\Gamma(m_{h_d})}\left(\frac{\Omega_{h_d}}{m_{h_d}}\right)^{\frac{3}{2}}B_r + m_{h_d}(m_{h_d}+1)\left(\frac{\Omega_{h_d}}{m_{h_d}}\right)^2. \quad \text{(A.21)}$$

This concludes the derivation of outage probability for UE$_r$.

Appendix B

Outage Probability of UE_t

$$
\begin{aligned}
P_t^{\text{out}} = \mathbb{P}\left\{R_t < R_t^{\text{th}}\right\} = \mathbb{P}\left\{\min(\gamma_{t\to r}, \gamma_{t\to t}) < \gamma_t^{\text{th}}\right\} = 1 \\
- \mathbb{P}\left\{\min(\gamma_{t\to r}, \gamma_{t\to t}) > \gamma_t^{\text{th}}\right\} = 1 - \mathbb{P}\left\{\gamma_{t\to r} > \gamma_t^{\text{th}}\right\} \\
\times \mathbb{P}\left\{\gamma_{t\to t} > \gamma_t^{\text{th}}\right\} = 1 - \left(1 - \mathbb{P}\left\{\gamma_{t\to r} < \gamma_t^{\text{th}}\right\}\right) \\
\times \left(1 - \mathbb{P}\left\{\gamma_{t\to t} < \gamma_t^{\text{th}}\right\}\right) = \mathbb{P}\left\{\gamma_{t\to r} < \gamma_t^{\text{th}}\right\} \\
+ \mathbb{P}\left\{\gamma_{t\to t} < \gamma_t^{\text{th}}\right\} - \mathbb{P}\left\{\gamma_{t\to r} < \gamma_t^{\text{th}}\right\} \times \mathbb{P}\left\{\gamma_{t\to t} < \gamma_t^{\text{th}}\right\}. \quad \text{(B.1)}
\end{aligned}
$$

Let us find first $\mathbb{P}\left\{\gamma_{t\to r} < \gamma_t^{\text{th}}\right\}$.

$$
\begin{aligned}
\mathbb{P}\left\{\gamma_{t\to r} < \gamma_t^{\text{th}}\right\} &= \mathbb{P}\left\{\frac{\rho\alpha_t\mathcal{G}_r}{\rho\alpha_r\mathcal{G}_r + ||\mathbf{g}_r^{\mathrm{H}}\mathbf{\Phi}_r||^2 + 1} < \gamma_t^{\text{th}}\right\} \\
&= \mathbb{P}\left\{\rho\mathcal{G}_r\left(\alpha_t - \alpha_r\gamma_t^{\text{th}}\right) - \left\|\mathbf{g}_r^{\mathrm{H}}\mathbf{\Phi}_r\right\|^2\gamma_t^{\text{th}} < \gamma_t^{\text{th}}\right\} \\
&= \mathbb{P}\left\{\frac{\mathcal{G}_r}{\gamma_t^{\text{th}}} - \frac{\left\|\mathbf{g}_r^{\mathrm{H}}\mathbf{\Phi}_r\right\|^2}{\rho\left(\alpha_t - \alpha_r\gamma_t^{\text{th}}\right)} < \frac{1}{\rho\left(\alpha_t - \alpha_r\gamma_t^{\text{th}}\right)}\right\} \\
&= \mathbb{P}\left\{\check{g}_r < \frac{1}{\rho\left(\alpha_t - \alpha_r\gamma_t^{\text{th}}\right)}\right\} = F_{\check{g}_r}\left(\frac{1}{\rho\left(\alpha_t - \alpha_r\gamma_t^{\text{th}}\right)}\right) \\
&= \frac{1}{\Gamma(k_{\check{g}_r})}\gamma\left(k_{\check{g}_r}, \frac{\frac{1}{\rho\left(\alpha_t - \alpha_r\gamma_t^{\text{th}}\right)}}{\theta_{\check{g}_r}}\right), \quad \text{(B.2)}
\end{aligned}
$$

where

$$
k_{\check{g}_r} = \frac{\mathbb{E}\left[\check{g}_r\right]^2}{\mathbb{V}\left[\check{g}_r\right]}, \quad \theta_{\check{g}_r} = \frac{\mathbb{V}\left[\check{g}_r\right]}{\mathbb{E}\left[\check{g}_r\right]}. \quad \text{(B.3)}
$$

$$\mathbb{E}\left[\breve{g}_r\right] = \mathbb{E}\left[\frac{\left(\sqrt{\beta_{max}}\sum_{m=1}^{M_r}\left(|g_r^{(m)}||h_r^{(m)}|\right)+|h_d|\right)^2}{\gamma_t^{\text{th}}}\right] - \frac{\beta_{\max}\sum_{m=1}^{M_r}|g_r^{(m)}|^2}{\rho\left(\alpha_t-\alpha_r\gamma_t^{\text{th}}\right)}$$

$$= \frac{1}{\gamma_t^{\text{th}}}\mathbb{E}\left[\left(\sqrt{\beta_{max}}\sum_{m=1}^{M_r}\left(|g_r^{(m)}||h_r^{(m)}|\right)+|h_d|\right)^2\right] - \frac{\beta_{\max}}{\rho\left(\alpha_t-\alpha_r\gamma_t^{\text{th}}\right)}\mathbb{E}\left[\sum_{m=1}^{M_r}|g_r^{(m)}|^2\right]$$

$$= \frac{1}{\gamma_t^{\text{th}}}\Bigg(\beta_{max}\underbrace{\mathbb{E}\left[\left(\sum_{m=1}^{M_r}|g_r^{(m)}||h_r^{(m)}|\right)^2\right]}_{A_r} + 2\sqrt{\beta_{max}}\mathbb{E}\left[|h_d|\right]\underbrace{\mathbb{E}\left[\sum_{m=1}^{M_r}\left(|g_r^{(m)}||h_r^{(m)}|\right)\right]}_{B_r} + \mathbb{E}\left[|h_d|^2\right]\Bigg) - \frac{\beta_{\max}}{\rho\left(\alpha_t-\alpha_r\gamma_t^{\text{th}}\right)}\sum_{m=1}^{M_r}\mathbb{E}\left[|g_r^{(m)}|^2\right] \quad \text{(B.4)}$$

$$\mathbb{E}\left[\breve{g}_r^2\right] = \mathbb{E}\left[\left(\frac{\left(\sqrt{\beta_{max}}\sum_{m=1}^{M_r}\left(|g_r^{(m)}||h_r^{(m)}|\right)+|h_d|\right)^2}{\gamma_t^{\text{th}}} - \frac{\beta_{\max}\sum_{m=1}^{M_r}|g_r^{(m)}|^2}{\rho\left(\alpha_t-\alpha_r\gamma_t^{\text{th}}\right)}\right)^2\right]$$

$$= \mathbb{E}\left[\frac{\left(\sqrt{\beta_{max}}\sum_{m=1}^{M_r}\left(|g_r^{(m)}||h_r^{(m)}|\right)+|h_d|\right)^4}{(\gamma_t^{\text{th}})^2}\right] - \mathbb{E}\left[\frac{2\beta_{\max}}{\gamma_t^{\text{th}}\rho\left(\alpha_t-\alpha_r\gamma_t^{\text{th}}\right)}\left(\sqrt{\beta_{\max}}\sum_{m=1}^{M_r}\left(|g_r^{(m)}||h_r^{(m)}|\right)+|h_d|\right)^2 \times\left(\sum_{m=1}^{M_r}|g_r^{(m)}|^2\right)\right] + \mathbb{E}\left[\frac{\beta_{\max}^2\left(\sum_{m=1}^{M_r}|g_r^{(m)}|^2\right)^2}{\left(\rho\left(\alpha_t-\alpha_r\gamma_t^{\text{th}}\right)\right)^2}\right], \quad \text{(B.5)}$$

which is

$$\mathbb{E}\left[\breve{g}_r^2\right] = \frac{1}{(\gamma_t^{\text{th}})^2}\Bigg(\beta_{\max}^2 C_r + 4\beta_{\max}^{\frac{3}{2}}\mu_{h_d}(1)D_r + 6\beta_{\max}\mu_{h_d}(2)A_r + 4\sqrt{\beta_{\max}}\mu_{h_d}(3)B_r + \mu_{h_d}(4)\Bigg) - \Bigg(\frac{2\beta_{\max}}{\gamma_t^{\text{th}}\rho\left(\alpha_t - \alpha_r\gamma_t^{\text{th}}\right)}\beta_{\max}E_r + 2\sqrt{\beta_{\max}}\mu_{h_d}(1)F_r + M_r\mu_{h_d}(2)\Bigg) + \frac{\beta_{\max}^2}{\left(\rho\left(\alpha_t - \alpha_r\gamma_t^{\text{th}}\right)\right)^2}H_r. \quad \text{(B.6)}$$

Now, in similar fashion, we can find $k_{\breve{g}_r}$ and $\theta_{\breve{g}_r}$. As for $\mathbb{P}\left\{\gamma_{t\to t} < \gamma_t^{\text{th}}\right\}$,

$$\begin{aligned}\mathbb{P}\left\{\gamma_{t\to t} < \gamma_t^{\text{th}}\right\} &= \mathbb{P}\left\{\frac{\rho\alpha_t\mathcal{G}_t}{\rho\alpha_r\mathcal{G}_t + \left|\left|\mathbf{g}_t^{\text{H}}\mathbf{\Phi}_t\right|\right|^2 + 1} < \gamma_t^{\text{th}}\right\} \\ &= \mathbb{P}\left\{\frac{\mathcal{G}_t}{\gamma_t^{\text{th}}} - \frac{\left\|\mathbf{g}_t^{\text{H}}\mathbf{\Phi}_t\right\|^2}{\rho\left(\alpha_t - \alpha_r\gamma_t^{\text{th}}\right)} < \frac{1}{\rho\left(\alpha_t - \alpha_r\gamma_t^{\text{th}}\right)}\right\} = \mathbb{P}\left\{\breve{g}_t < \frac{1}{\rho\left(\alpha_t - \alpha_r\gamma_t^{\text{th}}\right)}\right\} \\ &= F_{\breve{g}_t}\left(\frac{1}{\rho\left(\alpha_t - \alpha_r\gamma_t^{\text{th}}\right)}\right) = \frac{1}{\Gamma(k_{\breve{g}_t})}\gamma(k_{\breve{g}_t}, \frac{\frac{1}{\rho\left(\alpha_t - \alpha_r\gamma_t^{\text{th}}\right)}}{\theta_{\breve{g}_t}}), \quad \text{(B.7)}\end{aligned}$$

where

$$k_{\breve{g}_t} = \frac{\mathbb{E}\left[\breve{g}_t\right]^2}{\mathbb{V}\left[\breve{g}_t\right]}, \quad \theta_{\breve{g}_t} = \frac{\mathbb{V}\left[\breve{g}_t\right]}{\mathbb{E}\left[\breve{g}_t\right]}. \quad \text{(B.8)}$$

$$\begin{aligned}\mathbb{E}\left[\breve{g}_t\right] &= \mathbb{E}\left[\frac{\beta_{max}\left(\sum_{m=1}^{M_t}|g_t^{(m)}||h_t^{(m)}|\right)^2}{\gamma_t^{\text{th}}} - \frac{\beta_{\max}\sum_{m=1}^{M_t}|g_t^{(m)}|^2}{\rho\left(\alpha_t - \alpha_r\gamma_t^{\text{th}}\right)}\right] = \frac{\beta_{max}}{\gamma_t^{\text{th}}}A_t \\ &\quad - \frac{\beta_{\max}M_t\Omega_{g_t}}{\rho\left(\alpha_t - \alpha_r\gamma_t^{\text{th}}\right)} \\ &= \frac{\beta_{\max}}{\gamma_t^{\text{th}}}\left(M_t\Omega_{g_t}\Omega_h + M_t(M_t-1)\left(\frac{\Gamma(m_{g_t}+\frac{1}{2})}{\Gamma(m_{g_t})}\right)^2\left(\frac{\Omega_{g_t}}{m_{g_t}}\right)\left(\frac{\Gamma(m_h+\frac{1}{2})}{\Gamma(m_h)}\right)^2\left(\frac{\Omega_h}{m_h}\right)\right) \\ &\quad - \frac{\beta_{\max}M_t\Omega_{g_t}}{\rho\left(\alpha_t - \alpha_r\gamma_t^{\text{th}}\right)} \quad \text{(B.9)}\end{aligned}$$

$$\mathbb{E}\left[\breve{g}_t^2\right] = \mathbb{E}\left[\left(\frac{\beta_{\max}\left(\sum_{m=1}^{M_t}|g_t^{(m)}||h_t^{(m)}|\right)^2}{\gamma_t^{\text{th}}} - \frac{\beta_{\max}\sum_{m=1}^{M_t}|g_t^{(m)}|^2}{\rho\left(\alpha_t - \alpha_r\gamma_t^{\text{th}}\right)}\right)^2\right]$$

$$= \mathbb{E}\left[\frac{\beta_{\max}^2\left(\sum_{m=1}^{M_t}|g_t^{(m)}||h_t^{(m)}|\right)^4}{(\gamma_t^{\text{th}})^2}\right]$$

$$- \mathbb{E}\left[\frac{2\beta_{\max}^2}{\gamma_t^{\text{th}}\rho\left(\alpha_t - \alpha_r\gamma_t^{\text{th}}\right)}\left(\sum_{m=1}^{M_t}|g_t^{(m)}||h_t^{(m)}|\right)^2\left(\sum_{m=1}^{M_t}|g_t^{(m)}|^2\right)\right] + \mathbb{E}\left[\frac{\beta_{\max}^2\left(\sum_{m=1}^{M_t}|g_t^{(m)}|^2\right)^2}{\left(\rho\left(\alpha_t - \alpha_r\gamma_t^{\text{th}}\right)\right)^2}\right]$$

$$= \left(\frac{\beta_{\max}}{\gamma_t^{\text{th}}}\right)^2 \underbrace{\mathbb{E}\left[\left(\sum_{m=1}^{M_t}|g_t^{(m)}||h_t^{(m)}|\right)^4\right]}_{C_t}$$

$$- \frac{2\beta_{\max}^2}{\gamma_t^{\text{th}}\rho\left(\alpha_t - \alpha_r\gamma_t^{\text{th}}\right)} \underbrace{\mathbb{E}\left[\left(\sum_{m=1}^{M_t}|g_t^{(m)}||h_t^{(m)}|\right)^2\sum_{m=1}^{M_t}|g_t^{(m)}|^2\right]}_{E_t}$$

$$+ \frac{\beta_{\max}^2}{\left(\rho\left(\alpha_t - \alpha_r\gamma_t^{\text{th}}\right)\right)^2} \underbrace{\mathbb{E}\left[\left(\sum_{m=1}^{M_t}|g_t^{(m)}|^2\right)^2\right]}_{H_t}. \quad \text{(B.10)}$$

Then, we have $k_{\breve{g}_t}$ and $\theta_{\breve{g}_t}$.

Appendix C

Ergodic Rate of UE$_r$

$$R_r = \mathbb{E}\left[\log_2\left(1+\gamma_{r\to r}\right)\right] = \mathbb{E}\left[\log_2\left(1+\frac{\rho\alpha_r\mathcal{G}_r}{||\mathbf{g}_r^{\mathrm{H}}\mathbf{\Phi}_r||^2+1}\right)\right]$$
$$= \frac{1}{\ln 2}\left(\mathbb{E}\left[\ln\left(\rho\alpha_r\mathcal{G}_r+\left|\left|\mathbf{g}_r^{\mathrm{H}}\mathbf{\Phi}_r\right|\right|^2+1\right)\right]\right.$$
$$\left.-\,\mathbb{E}\left[\ln\left(\left|\left|\mathbf{g}_r^{\mathrm{H}}\mathbf{\Phi}_r\right|\right|^2+1\right)\right]\right). \quad \text{(C.1)}$$

A second-order Taylor series of $\ln x$ about $\mathbb{E}[x]$ is

$$\ln x = \ln\left(\mathbb{E}[x]\right) - \frac{\left(x-\mathbb{E}[x]\right)^2}{2\mathbb{E}[x]^2}. \quad \text{(C.2)}$$

Then,

$$\mathbb{E}[\ln x] = \ln\left(\mathbb{E}[x]\right) - \frac{\mathbb{V}[x]}{2\mathbb{E}[x]^2}. \quad \text{(C.3)}$$

Then,

$$R_r = \frac{1}{\ln 2}\left(\ln\left(\mathbb{E}\left[\rho\alpha_r\mathcal{G}_r+\left|\left|\mathbf{g}_r^{\mathrm{H}}\mathbf{\Phi}_r\right|\right|^2+1\right]\right) - \frac{\mathbb{V}\left[\rho\alpha_r\mathcal{G}_r+\left|\left|\mathbf{g}_r^{\mathrm{H}}\mathbf{\Phi}_r\right|\right|^2+1\right]}{2\mathbb{E}\left[\rho\alpha_r\mathcal{G}_r+||\mathbf{g}_r^{\mathrm{H}}\mathbf{\Phi}_r||^2+1\right]^2}\right.$$
$$\left.-\ln\left(\mathbb{E}\left[\left|\left|\mathbf{g}_r^{\mathrm{H}}\mathbf{\Phi}_r\right|\right|^2+1\right]\right) + \frac{\mathbb{V}\left[\left|\left|\mathbf{g}_r^{\mathrm{H}}\mathbf{\Phi}_r\right|\right|^2+1\right]}{2\mathbb{E}\left[||\mathbf{g}_r^{\mathrm{H}}\mathbf{\Phi}_r||^2+1\right]^2}\right) \quad \text{(C.4)}$$

Let us find $\mathbb{E}\left[\rho\alpha_r\mathcal{G}_r + \left|\left|\mathbf{g}_r^{\mathrm{H}}\mathbf{\Phi}_r\right|\right|^2 + 1\right]$ and $\mathbb{V}\left[\rho\alpha_r\mathcal{G}_r + \left|\left|\mathbf{g}_r^{\mathrm{H}}\mathbf{\Phi}_r\right|\right|^2 + 1\right]$.

$$K_r = \mathbb{E}\left[\rho\alpha_r\mathcal{G}_r + \left|\left|\mathbf{g}_r^{\mathrm{H}}\mathbf{\Phi}_r\right|\right|^2 + 1\right] = \mathbb{E}\left[\rho\alpha_r\mathcal{G}_r\right] + \mathbb{E}\left[\left|\left|\mathbf{g}_r^{\mathrm{H}}\mathbf{\Phi}_r\right|\right|^2\right] + 1 = \rho\alpha_r I_r + \beta_{\max}\mathbb{E}\left[\sum_{m=1}^{M_r}|g_r^{(m)}|^2\right] + 1 = \rho\alpha_r I_r + \beta_{\max}M_r\Omega_{g_r} + 1 \quad \text{(C.5)}$$

$$L_r = \mathbb{E}\left[\left(\rho\alpha_r\mathcal{G}_r + \left|\left|\mathbf{g}_r^{\mathrm{H}}\mathbf{\Phi}_r\right|\right|^2 + 1\right)^2\right] = \mathbb{E}\left[\left(\rho\alpha_r\mathcal{G}_r\right)^2 + \beta_{\max}^2\left(\sum_{m=1}^{M_r}|g_r^{(m)}|^2\right)^2 + 1 + 2\left(\rho\alpha_r\mathcal{G}_r\beta_{\max}\sum_{m=1}^{M_r}|g_r^{(m)}|^2 + \rho\alpha_r\mathcal{G}_r + \beta_{\max}\sum_{m=1}^{M_r}|g_r^{(m)}|^2\right)\right] = \left(\rho\alpha_r\right)^2 J_r + \beta_{\max}^2 H_r + 1 + 2\rho\alpha_r\left(\beta_{\max}M_r\Omega_{g_r} + 1\right) I_r + 2\beta_{\max}M_r\Omega_{g_r} \quad \text{(C.6)}$$

$$N_r = \mathbb{V}\left[\rho\alpha_r\mathcal{G}_r + \left|\left|\mathbf{g}_r^{\mathrm{H}}\mathbf{\Phi}_r\right|\right|^2 + 1\right] = \mathbb{E}\left[\left(\rho\alpha_r\mathcal{G}_r + \left|\left|\mathbf{g}_r^{\mathrm{H}}\mathbf{\Phi}_r\right|\right|^2 + 1\right)^2\right] - \mathbb{E}\left[\rho\alpha_r\mathcal{G}_r + \left|\left|\mathbf{g}_r^{\mathrm{H}}\mathbf{\Phi}_r\right|\right|^2 + 1\right]^2$$

$$\mathbb{E}\left[\left|\left|\mathbf{g}_r^{\mathrm{H}}\mathbf{\Phi}_r\right|\right|^2 + 1\right] = \beta_{\max}M_r\Omega_{g_r} + 1 \quad \text{(C.7)}$$

$$\mathbb{V}\left[\left|\left|\mathbf{g}_r^{\mathrm{H}}\mathbf{\Phi}_r\right|\right|^2 + 1\right] = \beta_{\max}^2\mathbb{V}\left[\sum_{m=1}^{M_r}|g_r^{(m)}|^2\right] = \beta_{\max}^2\sum_{m=1}^{M_r}\mathbb{V}\left[|g_r^{(m)}|^2\right] = \beta_{\max}^2 M_r m_{g_r}\left(\frac{\Omega_{g_r}}{m_{g_r}}\right)^2 = \frac{\beta_{\max}^2 M_r\Omega_{g_r}^2}{m_{g_r}} \quad \text{(C.8)}$$

Then,

$$R_r = \frac{1}{\ln 2}\left(\ln\left(K_r\right) - \frac{N_r}{2K_r^2} - \ln\left(\beta_{\max}M_r\Omega_{g_r} + 1\right) + \frac{\frac{\beta_{\max}^2 M_r\Omega_{g_r}^2}{m_{g_r}}}{2\left(\beta_{\max}M_r\Omega_{g_r} + 1\right)^2}\right). \quad \text{(C.9)}$$

Appendix D

Ergodic Rate of UE_t

$$R_t = \mathbb{E}\left[\min\left(\log_2\left(1+\gamma_{t\to r}\right), \log_2\left(1+\gamma_{t\to t}\right)\right)\right] = \min\left(\mathbb{E}\left[\log_2\left(1+\gamma_{t\to r}\right)\right], \mathbb{E}\left[\log_2\left(1+\gamma_{t\to t}\right)\right]\right) \quad \text{(D.1)}$$

$$\mathbb{E}\left[\log_2\left(1+\gamma_{t\to r}\right)\right] = \mathbb{E}\left[\log_2\left(1+\frac{\rho\alpha_t\mathcal{G}_r}{\rho\alpha_r\mathcal{G}_r+\left\|\mathbf{g}_r^{\mathrm{H}}\mathbf{\Phi}_r\right\|^2+1}\right)\right] = \frac{1}{\ln 2}\mathbb{E}\left[\ln\left(\frac{\rho\mathcal{G}_r+\left\|\mathbf{g}_r^{\mathrm{H}}\mathbf{\Phi}_r\right\|^2+1}{\rho\alpha_r\mathcal{G}_r+\left\|\mathbf{g}_r^{\mathrm{H}}\mathbf{\Phi}_r\right\|^2+1}\right)\right] = \frac{1}{\ln 2} \times \left(\mathbb{E}\left[\ln\left(\rho\mathcal{G}_r+\left\|\mathbf{g}_r^{\mathrm{H}}\mathbf{\Phi}_r\right\|^2+1\right)\right] - \mathbb{E}\left[\ln\left(\rho\alpha_r\mathcal{G}_r + \left\|\mathbf{g}_r^{\mathrm{H}}\mathbf{\Phi}_r\right\|^2+1\right)\right]\right)$$

$$O_r = \mathbb{E}\left[\left(\rho\mathcal{G}_r+\left\|\mathbf{g}_r^{\mathrm{H}}\mathbf{\Phi}_r\right\|^2+1\right)\right] = \rho I_r + \beta_{\max}M_r\Omega_{g_r}+1 \quad \text{(D.2)}$$

$$P_r = \mathbb{E}\left[\left(\rho\mathcal{G}_r+\left\|\mathbf{g}_r^{\mathrm{H}}\mathbf{\Phi}_r\right\|^2+1\right)^2\right] = \rho^2 J_r + \beta_{\max}^2 M_r\Omega_{g_r}+1 + 2\rho\left(\beta_{\max}M_r\Omega_{g_r}+1\right)I_r + 2\beta_{\max}M_r\Omega_{g_r} \quad \text{(D.3)}$$

$$Q_r = \mathbb{V}\left[\left(\rho\mathcal{G}_r+\left\|\mathbf{g}_r^{\mathrm{H}}\mathbf{\Phi}_r\right\|^2+1\right)\right] = \mathbb{E}\left[\left(\rho\mathcal{G}_r+\left\|\mathbf{g}_r^{\mathrm{H}}\mathbf{\Phi}_r\right\|^2+1\right)^2\right] - \mathbb{E}\left[\left(\rho\mathcal{G}_r+\left\|\mathbf{g}_r^{\mathrm{H}}\mathbf{\Phi}_r\right\|^2+1\right)\right]^2 \quad \text{(D.4)}$$

$$\mathbb{E}\left[\log_2\left(1+\gamma_{t\to r}\right)\right] = \frac{1}{\ln 2}\left(\ln\left(\mathbb{E}\left[\rho\mathcal{G}_r + \left|\left|\mathbf{g}_r^{\mathrm{H}}\mathbf{\Phi}_r\right|\right|^2 + 1\right]\right) - \frac{\mathbb{V}\left[\rho\mathcal{G}_r + \left|\left|\mathbf{g}_r^{\mathrm{H}}\mathbf{\Phi}_r\right|\right|^2 + 1\right]}{2\mathbb{E}\left[\rho\mathcal{G}_r + \left|\left|\mathbf{g}_r^{\mathrm{H}}\mathbf{\Phi}_r\right|\right|^2 + 1\right]^2} - \ln\left(\mathbb{E}\left[\rho\alpha_r\mathcal{G}_r + \left|\left|\mathbf{g}_r^{\mathrm{H}}\mathbf{\Phi}_r\right|\right|^2 + 1\right]\right) + \frac{\mathbb{V}\left[\rho\alpha_r\mathcal{G}_r + \left|\left|\mathbf{g}_r^{\mathrm{H}}\mathbf{\Phi}_r\right|\right|^2 + 1\right]}{2\mathbb{E}\left[\rho\alpha_r\mathcal{G}_r + \left|\left|\mathbf{g}_r^{\mathrm{H}}\mathbf{\Phi}_r\right|\right|^2 + 1\right]^2}\right)$$

$$\begin{aligned}\mathbb{E}\left[\log_2\left(1+\gamma_{t\to t}\right)\right] &= \mathbb{E}\left[\log_2\left(1+\frac{\rho\alpha_t\mathcal{G}_t}{\rho\alpha_r\mathcal{G}_t + \left\|\mathbf{g}_t^{\mathrm{H}}\mathbf{\Phi}_t\right\|^2 + 1}\right)\right] \\ &= \frac{1}{\ln 2}\mathbb{E}\left[\ln\left(\frac{\rho\mathcal{G}_t + \left\|\mathbf{g}_t^{\mathrm{H}}\mathbf{\Phi}_t\right\|^2 + 1}{\rho\alpha_r\mathcal{G}_t + \left\|\mathbf{g}_t^{\mathrm{H}}\mathbf{\Phi}_t\right\|^2 + 1}\right)\right] = \frac{1}{\ln 2} \\ &\times\left(\mathbb{E}\left[\ln\left(\rho\mathcal{G}_t + \left\|\mathbf{g}_t^{\mathrm{H}}\mathbf{\Phi}_t\right\|^2 + 1\right)\right] - \mathbb{E}\left[\ln\left(\rho\alpha_r\mathcal{G}_t + \left\|\mathbf{g}_t^{\mathrm{H}}\mathbf{\Phi}_t\right\|^2 + 1\right)\right]\right)\end{aligned}$$

$$\mathbb{E}\left[\left(\rho\mathcal{G}_t + \left\|\mathbf{g}_t^{\mathrm{H}}\mathbf{\Phi}_t\right\|^2 + 1\right)\right] = \rho\mathbb{E}\left[\mathcal{G}_t\right] + \beta_{\max}M_t\Omega_{g_t} + 1 \tag{D.5}$$

$$\begin{aligned}\mathbb{E}\left[\left(\rho\mathcal{G}_t + \left\|\mathbf{g}_t^{\mathrm{H}}\mathbf{\Phi}_t\right\|^2 + 1\right)^2\right] &= \rho^2\mathbb{E}\left[\mathcal{G}_t^2\right] + \beta_{\max}^2 G_t + 1 \\ &+ 2\rho\left(\beta_{\max}M_t\Omega_{g_t} + 1\right)\mathbb{E}\left[\mathcal{G}_t\right] + 2\beta_{\max}M_t\Omega_{g_t}\end{aligned} \tag{D.6}$$

$$\begin{aligned}\mathbb{V}\left[\left(\rho\mathcal{G}_t + \left\|\mathbf{g}_t^{\mathrm{H}}\mathbf{\Phi}_t\right\|^2 + 1\right)\right] &= \mathbb{E}\left[\left(\rho\mathcal{G}_t + \left\|\mathbf{g}_t^{\mathrm{H}}\mathbf{\Phi}_t\right\|^2 + 1\right)^2\right] \\ &- \mathbb{E}\left[\left(\rho\mathcal{G}_t + \left\|\mathbf{g}_t^{\mathrm{H}}\mathbf{\Phi}_t\right\|^2 + 1\right)\right]^2\end{aligned} \tag{D.7}$$

$$\mathbb{E}\left[\log_2\left(1+\gamma_{t\to t}\right)\right] = \frac{1}{\ln 2}\left(\ln\left(\mathbb{E}\left[\rho\mathcal{G}_t + \left|\left|\mathbf{g}_t^{\mathrm{H}}\mathbf{\Phi}_t\right|\right|^2 + 1\right]\right) - \frac{\mathbb{V}\left[\rho\mathcal{G}_t + \left|\left|\mathbf{g}_t^{\mathrm{H}}\mathbf{\Phi}_t\right|\right|^2 + 1\right]}{2\mathbb{E}\left[\rho\mathcal{G}_t + \left|\left|\mathbf{g}_t^{\mathrm{H}}\mathbf{\Phi}_t\right|\right|^2 + 1\right]^2} - \ln\left(\mathbb{E}\left[\rho\alpha_r\mathcal{G}_t + \left|\left|\mathbf{g}_t^{\mathrm{H}}\mathbf{\Phi}_t\right|\right|^2 + 1\right]\right) + \frac{\mathbb{V}\left[\rho\alpha_r\mathcal{G}_t + \left|\left|\mathbf{g}_t^{\mathrm{H}}\mathbf{\Phi}_t\right|\right|^2 + 1\right]}{2\mathbb{E}\left[\rho\alpha_r\mathcal{G}_t + \left|\left|\mathbf{g}_t^{\mathrm{H}}\mathbf{\Phi}_t\right|\right|^2 + 1\right]^2}\right) \quad \text{(D.8)}$$